



Deposited via The University of Sheffield.

White Rose Research Online URL for this paper:

<https://eprints.whiterose.ac.uk/id/eprint/241132/>

Version: Published Version

---

**Article:**

Harper, N.S., Sharpe, J.L., Speranza, J. et al. (2026) Targeting the integrated stress response or Ataxin-2 alleviates neurodegeneration in PolyGR models of C9orf72 associated frontotemporal dementia and amyotrophic lateral sclerosis. *Acta Neuropathologica Communications*. ISSN: 2051-5960

<https://doi.org/10.1186/s40478-026-02301-2>

---

**Reuse**

This article is distributed under the terms of the Creative Commons Attribution (CC BY) licence. This licence allows you to distribute, remix, tweak, and build upon the work, even commercially, as long as you credit the authors for the original work. More information and the full terms of the licence here:

<https://creativecommons.org/licenses/>

**Takedown**

If you consider content in White Rose Research Online to be in breach of UK law, please notify us by emailing [eprints@whiterose.ac.uk](mailto:eprints@whiterose.ac.uk) including the URL of the record and the reason for the withdrawal request.

# Targeting the integrated stress response or Ataxin-2 alleviates neurodegeneration in PolyGR models of C9orf72 associated frontotemporal dementia and amyotrophic lateral sclerosis

Received: 19 June 2025

Accepted: 17 April 2026

Published online: 05 May 2026

Cite this article as: Harper N.S., Sharpe J.L., Speranza J. *et al.* Targeting the integrated stress response or Ataxin-2 alleviates neurodegeneration in PolyGR models of C9orf72 associated frontotemporal dementia and amyotrophic lateral sclerosis. *acta neuropathol commun* (2026). <https://doi.org/10.1186/s40478-026-02301-2>

Nikki S. Harper, Joanne L. Sharpe, Jasmine Speranza, Ravinder Gulia, Jeffrey X. Chen, Scott P. Allen, Manpreet S. Atwal, Stuart Pickering-Brown, Matthew R. Livesey, Craig L. Bennett, Andreas Prokop, Albert R. La Spada & Ryan J. H. West

We are providing an unedited version of this manuscript to give early access to its findings. Before final publication, the manuscript will undergo further editing. Please note there may be errors present which affect the content, and all legal disclaimers apply.

If this paper is publishing under a Transparent Peer Review model then Peer Review reports will publish with the final article.

## Targeting the Integrated Stress Response or Ataxin-2 alleviates Neurodegeneration in PolyGR models of C9orf72 associated Frontotemporal Dementia and Amyotrophic Lateral Sclerosis

Nikki S. Harper <sup>1</sup>, Joanne L. Sharpe <sup>2,3\*</sup>, Jasmine Speranza <sup>2,3\*</sup>, Ravinder Gulia <sup>4</sup>, Jeffrey X. Chen <sup>4</sup>, Scott P. Allen <sup>2,3</sup>, Manpreet S. Atwal <sup>2,3</sup>, Stuart Pickering-Brown <sup>1</sup>, Matthew R. Livesey <sup>2,3</sup>, Craig L. Bennett <sup>4,5</sup>, Andreas Prokop <sup>6</sup>, Albert R. La Spada <sup>4,5,7,8,9</sup>, Ryan J. H. West <sup>2,3</sup>

<sup>1</sup> Division of Neuroscience and Experimental Psychology, Faculty of Biology, Medicine and Health, University of Manchester, Manchester, UK

<sup>2</sup> Sheffield Institute for Translational Neuroscience (SITraN), University of Sheffield, 385a Glossop Road, Sheffield, S10 2HQ, UK

<sup>3</sup> Neuroscience Institute, University of Sheffield, Sheffield, S10 2TN, UK

<sup>4</sup> Department of Pathology and Laboratory Medicine, University of California, Irvine, Irvine, CA, 92617, USA

<sup>5</sup> UCI Center for Neurotherapeutics, University of California, Irvine; Irvine, CA 92697, USA

<sup>6</sup> Division of Molecular and Cellular Function, Faculty of Biology, Medicine and Health, The University of Manchester, Manchester, UK

<sup>7</sup> Department of Biological Chemistry, University of California Irvine, Irvine, CA 92617, USA.

<sup>8</sup> Department of Neurology, University of California, Irvine, Irvine, CA 92617, USA

<sup>9</sup> Department of Neurobiology and Behavior, University of California Irvine, Irvine, CA 92697, USA.

\* These authors contributed equally

Corresponding Author

Dr Ryan J. H. West

[r.j.west@sheffield.ac.uk](mailto:r.j.west@sheffield.ac.uk)

Tel: +44 (0)114 222 2239

**Abstract**

Frontotemporal dementia (FTD) and amyotrophic lateral sclerosis (ALS) are fatal, early-onset neurodegenerative diseases. The most common genetic cause of FTD and ALS is a G4C2 hexanucleotide repeat expansion in the *C9orf72* gene. This mutation leads to the production of toxic dipeptide repeat proteins (DPRs), via repeat-associated non-AUG (RAN) translation. These DPRs disrupt stress granule (SG) dynamics, with SG regulators such as Ataxin-2 (ATXN2) implicated in disease risk. The integrated stress response (ISR), a key driver of SG formation via eIF2 $\alpha$  phosphorylation, has been linked to *C9orf72* expansions, but the role of individual DPRs in ISR activation remains unclear. Here, using *Drosophila* models expressing physiologically relevant repeat length DPRs, we identify poly(GR) as a novel activator of the ISR, inducing early and sustained eIF2 $\alpha$  phosphorylation and SG accumulation prior to motor decline. Genetic inhibition of the ISR or knockdown of *ATXN2*, the *Drosophila* orthologue of *ATXN2*, rescues motor deficits in these models. *ATXN2* knockdown also reduces poly(GR) toxicity in mouse primary neurons. These findings position poly(GR) as a key driver of ISR activation and highlight *ATXN2* and the ISR as promising therapeutic targets in *C9orf72*-associated FTD/ALS.

**Keywords**

C9orf72, Frontotemporal Dementia, Ataxin-2, Amyotrophic Lateral Sclerosis, Motor Neurone Disease integrated stress response, stress granules, *Drosophila*

## Introduction

Frontotemporal dementia (FTD) and amyotrophic lateral sclerosis (ALS) are two devastating early onset neurodegenerative diseases, for which there is currently no cure. FTD is characterised by the progressive degeneration of the frontal and temporal lobes of the brain leading to severe behavioural and language impairments. In contrast, ALS is hallmarked by upper and lower motor neuron loss resulting in debilitating motor deficits. The two conditions share a clinical, pathological and genetic spectrum, with the most common genetic cause of both FTD and ALS being a hexanucleotide (G<sub>4</sub>C<sub>2</sub>) repeat expansion mutation within the *C9orf72* gene [12, 36]. Both loss-of-function, through *C9orf72* haploinsufficiency, and gain-of-function mechanisms have been proposed to explain how *C9orf72* expansions contribute to disease. However, it is the bidirectional repeat-associated non-AUG (RAN) translation of sense and antisense *C9orf72* repeat RNA, facilitating the synthesis of five dipeptide repeat proteins (DPRs), that is thought to be the most prominent driver of neurodegeneration in *C9orf72*-FTD/ALS [5, 31, 49]. The five DPRs comprise poly-proline-alanine (AP), poly-proline-arginine (PR), poly-glycine-arginine (GR), poly-glycine-alanine (GA) and poly-glycine-proline (GP).

DPRs aggregate within neurons and have been implicated in the disruption of a range of cellular processes, including stress granule dynamics [26, 51]. The arginine-rich DPRs, GR and PR, have been shown to enhance the formation of stress granules, impair their disassembly and form pathological aggregates that colocalise with, and promote the phase separation of, several stress granule-associated RNA-binding proteins. These include Tia1 cytotoxic granule-associated RNA binding protein (TIA1), G3BP Stress Granule Assembly Factor 1 (G3BP1) and Ataxin-2 (ATXN2) [7, 21, 26, 45, 51]. Stress granule formation occurs, in part, following phosphorylation and activation of eukaryotic initiation factor 2 $\alpha$  (eIF2 $\alpha$ ).

eIF2 $\alpha$  is a core component of the integrated stress response (ISR), a regulatory pathway that maintains cellular homeostasis in response to physiological and pathological stress stimuli. Increasing evidence implicates both the ISR and dysregulated stress granule dynamics in the pathogenesis of ALS and FTD [10, 15, 18, 20, 33, 40, 50, 51]. C9orf72 expansions have been associated with activation of the ISR, with increased stress granule formation and eIF2 $\alpha$  phosphorylation observed in C9orf72 patient-derived cell models and patient tissue [18, 20, 33, 40, 50, 51]. Previous work has also demonstrated that RAN translation of C9orf72 repeat RNA requires an eIF2 $\alpha$  phosphorylation-dependent alteration in start codon fidelity [10, 15]. This suggests that RAN translation, and therefore DPR synthesis, is selectively enhanced by activation of the ISR. If DPRs independently induce cellular stress, promote chronic activation of the ISR and enhance the aberrant formation and persistence of stress granules, this may in turn contribute to a potential positive feedback loop, driving a neurotoxic cascade. Despite this, mechanisms leading to eIF2 $\alpha$  phosphorylation, and whether it is underpinned by specific DPR species remains unclear.

In this study we have utilised our *Drosophila* models, which individually express each DPR at a length that is pathologically and physiologically comparable to the longest repeat lengths observed in patients (>1000 repeats), to show that pan-neuronal expression of 1000-repeat GR promotes eIF2 $\alpha$  phosphorylation and stress granule accumulation. eIF2 $\alpha$  phosphorylation occurs early, preceding motor decline, suggesting a sustained and chronic activation of the ISR. Furthermore, we show that targeted inhibition of the ISR or knockdown of the *Drosophila* ATXN2 orthologue, *ATX2*, a key regulator of stress granule formation, is sufficient to rescue motor dysfunction in these models. Finally, we reveal knockdown of *ATXN2* is sufficient to reduce toxicity in mouse primary neurons transduced with PolyGR. These findings reveal ATXN2, and the ISR, to be potential therapeutic targets for the treatment of FTD and ALS associated with C9orf72 hexanucleotide expansions.

## Methods

### *Drosophila* stocks and maintenance

Unless stated otherwise *Drosophila* were raised on standard cornmeal-yeast medium (7.2 % w/v maize flour, 5 % w/v yeast, 8 % w/v glucose, 0.8 % w/v agar) at 25 °C on a 12 h light:dark cycle. UAS-AP(1024)-eGFP (Flybase ID Fbti0213155), UAS-PR(1100)-eGFP (Flybase ID Fbti0213157), UAS-GA(1020)-eGFP (Flybase ID Fbti0213158), and UAS-GR(1136)-eGFP (Flybase ID Fbti0213156), referred to throughout as 1000 repeat lines, were described previously [49]. nSyb-Gal4 (II) was described previously [49]. GMR-Gal4 (RRID:BDSC\_9146), UAS-mCD8-GFP (RRID:BDSC\_32184), UAS-PPP1R15 (RRID:BDSC\_76250), UAS-mCherry-RNAi (RRID:BDSC\_35785), UAS-ATX2-RNAi<sup>2</sup> (ATX2<sup>HMS02726</sup>, RRID:BDSC\_44012), UAS-ATXN2.22Q (RRID:BDSC\_79594), UAS-ATXN2.32Q (RRID:BDSC\_79593), UAS-GCN2-RNAi<sup>1</sup> (GCN2<sup>HMC06316</sup>, RRID:BDSC\_67215), UAS-PEK-RNAi (PEK<sup>HMJ02063</sup>, RRID:BDSC\_42499) and PEK<sup>e01744</sup> (RRID:BDSC\_85557) were obtained from the Bloomington *Drosophila* Stock Center (BDSC). UAS-ATX2 (FlyORF: F001031) was obtained from the FlyORF Zurich ORFeome stock center [6]. UAS-ATX2-RNAi<sup>1</sup> (ATX2<sup>GD11562</sup>, VDRC ID: 34955) and UAS-GCN2-RNAi<sup>2</sup> (GCN2<sup>GD9162</sup>, VDRC ID: 32664) were obtained from the Vienna *Drosophila* Resource Center (VDRC). Wild-types are Canton S outcrossed to *w*<sup>1118</sup>. All experiments were performed using flies from at least 3 independent crosses.

### **SDS-PAGE and Western blotting**

Flies pan-neuronally (nSyb-Gal4) expressing either UAS-AP(1000), UAS-GA(1000), UAS-PR(1000), UAS-GR(1000) or UAS-mCD8-GFP controls were snap frozen on dry ice and heads removed by vortexing, as described previously [42]. 20-40 heads, per genotype, per repeat, were lysed in RIPA buffer (10 mM Tris-Cl pH 8.0, 1 mM EDTA, 0.5 mM EGTA, 1 % Triton X-100, 0.1 % Sodium deoxycholate, 0.1 % SDS, 140 mM NaCl) containing Halt™ Protease and Phosphatase Inhibitor Cocktail, EDTA-free (100X) (Thermo Fisher #78441). Lysates were cleared by centrifugation (15-minutes 13,000 rpm), concentrations quantified using A Pierce™ BCA Protein Assay Kit (Thermo Fisher #23227) and diluted to equal concentrations. Lysates were mixed with Laemmli buffer (20 µg total protein, 2 % SDS, 10 % glycerol, 60 mM Tris-CL pH 6.8, 0.01 % bromophenol blue, 20 mM DTT) and run on 12 % SDS-PAGE gels. Transfers were performed for 1 h (100 V, 20% Methanol, Hybond-

P polyvinylidene difluoride (PVDF) membrane (Amersham #RNP1416F)). Primary antibodies used were anti-EIF2S1 (Abcam Cat# ab26197, RRID:AB\_2096478, Rabbit, 1:1000), anti-EIF2S1 (phospho S51) (Abcam Cat# ab32157, RRID:AB\_732117, Rabbit, 1:1000), anti-ATX2 (Chicken, 1:1000, A gift from Prof. Mani Ramaswami, Trinity College, Dublin [2]), anti- $\alpha$ -tubulin (Sigma-Aldrich Cat# T9026, RRID:AB\_477593, Mouse, 1:4000) and anti-beta-tubulin (DSHB Cat# E7, RRID:AB\_528499, mouse, 1:5000). All primary antibody incubations were performed at 4 °C overnight. Secondary antibodies were goat anti-rabbit-HRP (Agilent Cat# P0448, RRID:AB\_2617138, 1:1000), goat anti-mouse-HRP (Agilent Cat# P0447, RRID:AB\_2617137, 1:1000), goat anti-chicken-HRP (Jackson ImmunoResearch Labs Cat# 103-035-155, RRID:AB\_2337381, 1:25,000), donkey anti-rabbit Alexa Fluor 790 (Jackson ImmunoResearch abs Cat# 711-655-152, AB\_2340628, 1:25,000) and donkey anti-mouse 800CW (LICORbio Cat# 926-32212, RRID:AB\_621847, 1:25,000). Secondary antibody incubations were performed for 1h at room temperature. Detection was performed using enhanced chemiluminescence substrate (ECL, Promega W1015) imaged on a G:box imaging unit (Syngene) with ECL settings or using a LICORbio Osysey Classic Imager. Western blots were quantified using ImageJ.

### **Negative geotaxis motor assays**

Without anaesthetisation, 5-10 male flies were placed in glass boiling tubes, mounted onto a custom-made apparatus with a white background. After acclimatisation, the apparatus was banged down three times in a consistent manner, causing the flies to elicit a startle-induced negative geotaxis escape response. A Konig Full HD Action camera recorded the flies as they climbed, for a maximum of 60 seconds, or until all flies reached the top of the tube. Videos were processed and analysed using ImageJ. Briefly, a custom macro was used to threshold the images, distinguishing each fly and excluding the background. The Mtrack2 plugin tracked the movement of individual flies between frames (30 frames per second). The relative position of each individual fly during a 15 second period was used to calculate the median climbing speed. Assays were carried out at 25 °C and at the same time each day, with a half-hour window, to mitigate the impact of circadian differences. For all assays, expression of constructs was driven using pan-neuronal nSyb-Gal4, on the

second chromosome. 20-30 flies per genotype were assessed from a minimum of three independent crosses.

### **Activity monitoring assays**

The TriKinetics *Drosophila* Activity Monitor 10 (DAM10) system was used to measure the activity of *Drosophila*, by recording infra-red beam breaks caused by the movement of the fly. Anaesthetised flies were placed in transparent tubes, supplied with food and sealed with a rubber bung at one end and secured with cotton wool at the other. Up to 32 tubes were loaded into the monitor at any given time. The monitor was housed in an incubator, maintained at 25 °C with constant humidity and subject to 12-hour light dark cycles. Flies were given 24 hours to acclimatise and recover from the CO<sub>2</sub> anaesthetisation, before activity was recorded. The locomotor activity of *Drosophila* was measured over 24 hours. The DAM10 TriKinetics software read at 30 second intervals across all four infra-red channels. A 'move' was registered each time a fly entered an infra-red beam after exiting another, preventing continuous movement around a single beam from being recorded. The DAMFileScan113 software was used to quantify the number of 'moves' in 24 hours.

### **Genetic interaction eye screens**

The glass multimer reporter (*GMR*)-*Gal4* line was used to drive expression of the 1000 repeat UAS-DPR constructs and the UAS-Ataxin-2 constructs, within the fly eye. For genetic interaction experiments flies were maintained at 29°C. Eye phenotypes were examined under a stereo microscope, within 3 days post-eclosion and imaged using a Leica MZ10F microscope with a Leica DFC410 C camera and Leica LAS software. Flies were taken from a minimum of 3 crosses per genotype, with at least 100 flies scored per genotype.

### **Seizure assays**

Mechanical induced seizure assays were performed as described previously [30]. Briefly ~ 5-6 flies were placed into an empty, transparent *Drosophila* food vial and vortexed using a Vortex-genie 2 lab vortex (Scientific Industries Inc) at the maximum speed setting (10)

for 10 seconds. Immediately following vortexing, video recordings were made of flies until all had recovered. Videos were analysed for the presence or absence, and length of, seizures using ImageJ.

### ***Drosophila* primary cell culture**

Primary neurons were cultured following protocols described previously [34, 35, 38, 49]. Briefly, embryos were dechorinated with 50 % bleach and selected at stage 11. Embryos were sterilised in 70 % ethanol, then washed in Schneider's medium, supplemented with 20 % foetal bovine serum. Embryos were mechanically and chemically dispersed in dispersion medium (0.002 g Collagenase Type 1, 0.004 g Dispase II, Hank's Balanced Salt Solution) and left to incubate for 5 minutes at 37 °C. After centrifugation, the pellet was washed and resuspended in Schneider's medium, then plated onto concanavalin A (5 µg/ml) coated glass coverslips. Cells were grown as hanging drop cultures, using custom chambers, and incubated at 26 °C for 5 days *in vitro*. Primary neurons were fixed in 4 % paraformaldehyde (PFA) in 0.05 M PBS (pH 7-7.2) for 30 minutes, then washed three times in PBS with 0.3 % Triton X-100 (PBS-T) prior to antibody staining. Primary antibodies were anti-tubulin (clone YL 1/2, Sigma-Aldrich, RRID:AB\_2890657, rat, 1:500), anti-dFMR1 (5A11, DSHB, RRID:AB\_528252, mouse, 1:20), anti-GFP (Alexa Fluor 488-conjugated, ChromoTek, RRID AB\_2827573, alpaca, 1:1000), anti-GFP (ab6556, abcam, RRID:AB\_305564, rabbit, 1:500), anti-HRP (Cy3 conjugated, Stratech, RRID AB\_2338959, goat, 1:200) and anti-eIF4E (Santa Cruz Biotechnology Cat# sc-9976, RRID:AB\_627502, mouse, 1:50). Secondary antibodies were Cy3 conjugated anti-Rat (Jackson ImmunoResearch, RRID: AB\_2340667, donkey, 1:200), anti-Mouse Alexa Fluor 647 (Jackson ImmunoResearch, RRID: AB\_2340863, donkey, 1:500) and FITC conjugated anti-Rabbit (Jackson ImmunoResearch, RRID: AB\_2315776, donkey, 1:500). Coverslips were mounted on slides using ProLong Gold and imaged using an Olympus BX50WI microscope, at 100X magnification, using Carl Zeiss™ Immersol™ Immersion Oil (518 N). For sodium arsenite treatment coverslips containing the hanging-drop cultures were removed from the chamber slides on the day of fixation (day 5 in culture) and the remaining growth media removed from the chamber. Chambers were briefly washed with 50 µl 0.5 mM NaAsO<sub>2</sub> (Thermo Fisher #AA41533AP) diluted in

growth media. 50  $\mu$ l of the 0.5 mM NaAsO<sub>2</sub> diluted in growth media was then added to each chamber and the coverslip replaced on its respective slide. Slides were returned to 26 °C for 180 minutes before the coverslips were removed, washed and fixed in 4% paraformaldehyde (PFA) in 0.05 M PBS, as above.

### **Brain dissection and immunohistochemistry**

*Drosophila* adult brains were dissected in PBS (137 mM NaCl, 2.7 mM KCl, 10 mM Na<sub>2</sub>HPO<sub>4</sub> and 1.8 mM KH<sub>2</sub>PO<sub>4</sub> in dH<sub>2</sub>O) on a sylgard plate (Silicone elastomere kit, DowCorning, MI, USA) prior to fixation in 3.7 % formaldehyde (FA, Sigma #252549) in PBS for 1 hour. Following three washes in 0.5 % PBS-T (0.5 % triton X-100 in PBS (v/v)) brains were incubated in primary antibodies anti-dFMR1 (5A11, DSHB, RRID:AB\_528252, mouse, 1:20) and anti-ATX2 (Chicken, 1:500, A gift from Prof. Mani Ramaswami, Trinity College, Dublin [2]) in 0.5 % PBS-T overnight, at 4 °C, with rotation. After incubation, brains were washed three times in 0.5 % PBS-T, then incubated with secondary antibodies anti-Chicken Alexa Fluor 647 (Jackson ImmunoResearch, RRID: AB\_2340379, Donkey, 1:500) and Cy3-conjugated anti-mouse (Jackson ImmunoResearch, RRID:AB\_2315777, Donkey, 1:500) in 0.5 % PBS-T for 1 hour at room temperature, in darkness, with rotation. Brains were washed three times in 0.5 % PBS-T and mounted using Vectashield® hard set mounting media (Vector Laboratories LTD, UK #H-1400-10) before imaging using either a Leica CTR6000 or EVOS M5000 widefield fluorescence microscope. Identical microscope settings were for all samples. Quantification of FMR1 and ATX2 puncta was performed in a define 5800  $\mu$ m<sup>2</sup> region of interest within the protocerbrum, imaged using either a 40x or 63X oil objective, using the same stack depth and slice-interval. Z-stack image were blinded, subjected to the background subtraction (rolling ball radius of 50 pixels) and a threshold applied equally prior to manual quantification. 3 individual regions of interest were quantified per brain and the mean taken. For heat stress experiments flies were placed at 37 °C for 2 hours before dissection.

### **iPSC-derived motor neurons**

Induced pluripotent stem cell (iPSC) lines CS28iALS-C9nxx (RRID:CVCL\_W558) and CS29iALS-C9nxx (RRID:CVCL\_W559), described and characterised previously, were obtained from Cedars-Sinai iPSC Biorepository [1, 9]. iPSCs were maintained at 37 °C and 5 % CO<sub>2</sub> in Matrigel-coated (Corning) 6-well plastic dishes in mTeSR™ medium (StemCell Technologies). Media was replaced every 2 days. iPSC to motor neuron differentiation was performed by adapting an established protocol [13]. iPSC lines at 100% confluency were switched to a default base media containing Knockout™ DMEM/F12 media (48 % v/v, Gibco), Neurobasal (48 % v/v, Gibco), B-27 supplement (1 % v/v, Gibco), Glutamax™ (1 % v/v, Gibco), N-2 supplement (0.5 % v/v, Gibco), penicillin/streptomycin (1 % v/v, Lonza). From 1 - 6 days the default media was supplemented with CHIR99021 (3 μM, Merck Millipore), DMH-1 (2 μM, Merck Millipore) and SB431542 (2 μM, Peprotech) to promote neural induction. On day 7, cultures were switched to a media, consisting of the former default media supplemented with the addition of retinoic acid (0.1 μM, StemCell Technologies) and purmorphamine (0.5 μM, Merck Millipore). Between day 7-9, cells were passaged using Accutase and replated onto Matrigel-coated 6-well plates. On day 12, NPCs were passaged, replated, and further maintained/expanded in the prior media additionally supplemented with valproic acid (0.5 μM, Merck Millipore). Media changes were performed every 24 hours until the NPC expansion stage. At 100 % confluence, NPCs were transitioned to motor neuron differentiation media, comprising the base media supplemented with retinoic acid (0.5 μM) and purmorphamine (0.1 μM). At day 19, cultures were maintained in the former media, but with further supplements of Compound-E (0.1 μM, StemCell Technologies), BDNF (10 ng/mL), CNTF (10 ng/mL, Peprotech) and IGF-1 (10 ng/mL, Peprotech). On days 20-21, the cultures were resuspended and replated onto Matrigel-coated 13 mm glass coverslips supplemented with Y27632 (10 μM). Fresh medium was added 24 hours after replating and changed every 48 hours thereafter. On day 29, cultures were maintained in a media comprising Neurobasal media, B-27 supplement (2% v/v), penicillin/Streptomycin (1 % v/v), BDNF (10 ng/ml), CNTF (10 ng/ml) and IGF-1 (10 ng/ml) until experimental use. Cells were stained with anti-GR (Millipore, Cat# MABN778, RRID:AB\_2728664, Rat 1:500), CoraLite Plus 488-conjugated anti-ATXN2 (Proteintech, Cat# CL488-68316, RRID:AB\_3084472, Mouse 1:500) and CoraLite Plus 647-

conjugated anti-G3BP1 (Proteintech, Cat# CL647-66486, RRID:AB\_2935056, Mouse 1:500) overnight, at 4 °C. Secondary antibodies were anti-Rat (Jackson ImmunoResearch, RRID: AB\_2340667, Donkey, 1:500) in 0.5 % PBS-T for 1 hour at room temperature, in darkness, with agitation. Coverslips were mounted in Vectashield® mounting media with DAPI (Vector Laboratories LTD, UK #H-1200) and imaged using an Opera Phenix high-content imaging system. Colocalization analysis was performed using the Coloc2 plugin in Fiji. Following automatic thresholding using the Costes threshold regression, the degree of spatial co-occurrence and signal correlation were quantified using thresholded Manders' overlap coefficients (tM1 and tM2) and thresholded Pearson's correlation coefficient (R), respectively. To verify that the observed colocalization was statistically significant and not due to random spatial overlap, Costes randomization was performed using 100 iterations and a point spread function (PSF) estimate of 3 pixels

### **Mouse primary neurons**

Primary cortical neurons (PCNs) were prepared from P0/P1 C57BL/6J mouse pups. Following euthanasia, cortices were dissected, and tissues were dissociated using an enzymatic solution containing papain for 30 minutes at 37 °C. Papain activity was then inactivated with serum-containing media. Cells were triturated with a pipette to obtain single-cell suspensions, and neurons plated on pre-coated coverslips (50 µg/mL poly-D-lysine + 0.1 M sodium borate, pH 8.4) at a density of ~70,000 cells per well in clear-bottom 96-well plates. Cultures were maintained in Neurobasal medium supplemented with 0.5 mM glutamine and B27. At day 3 Glial growth was inhibited by adding FUDR (floxuridine) to the culture. At day 6 lentivirus containing shRNA sequences for Scramble or Atxn2 (VB900142-8349skf) were added at a Multiplicity of Infection (MOI) of 5. At day 8 AAVs expressing GFP, GR100, and GR200 (generously provided by Leonard Petrucelli [11]) were applied at a MOI of 50,000. PCNs were fixed (Day 15) in 4% PFA, permeabilised with 0.1% Triton X-100 and incubated with anti-MAP2 polyclonal antibody (Thermo Fisher Scientific Cat# PA1-10005, RRID:AB\_1076848, Chicken, 1:500) at 4°C overnight. PCNs were washed with PBS and incubated with a secondary antibody (Thermo Fisher Scientific Cat# A32932, RRID:AB\_2762844, Goat) for 1 hour at room temperature. Finally, PCNs were stained with

Hoechst (1:10,000 dilution, H1399, Fisher Scientific) and imaged using a Nikon AR confocal microscope (20X objective). Sholl analysis was performed using the Sholl plugin in Fiji [41].

## Results

### **1000-repeat polyGR leads to an increase in eIF2 $\gamma$ phosphorylation in the *Drosophila* nervous system**

Aberrantly increased phosphorylation of the ISR master regulator eIF2 $\gamma$  has previously been observed in C9orf72 repeat expansion patient tissues, and patient-derived cell models [18, 20, 33, 40, 50, 51]. P-eIF2 $\gamma$  dependent activation of the ISR has also been shown to promote RAN translation, leading to increased DPR production, which may in turn activate the ISR in a pathological feedback loop [16]. We hypothesise this leads to chronic activation of the ISR, which has previously been shown to cause neurodegeneration (reviewed in Bond et al., 2020 [8]). Despite this, it is unclear how C9orf72 hexanucleotide repeats lead to eIF2 $\gamma$  phosphorylation and whether this is driven by specific DPR species. To explore this we utilised our previously characterised *Drosophila* models expressing 1000-repeat DPRs to examine eIF2 $\gamma$  phosphorylation state at time points previously shown to be pre- and post-motor decline (7- and 21-days post eclosion) [4, 48, 49]. Pan-neuronal (nSyb-Gal4) expression of AP(1000), PR(1000), GR(1000) or GA(1000) had no significant effect on the abundance of total eIF2 $\gamma$  in the brains of flies at 7 or 21 days post-eclosion, when compared to controls (Fig. 1a, b, c). While pan-neuronal expression of AP(1000), PR(1000), or GA(1000) also showed no significant difference in the levels of p-eIF2 $\gamma$ , compared to controls, pan-neuronal expression of GR(1000) led to a significant increase in the abundance of p-eIF2 $\gamma$  in the brains of flies at both 7 ( $p = 0.0003$ ) and 21 days post eclosion ( $p = 0.0045$ ) (Fig. 1a, d, e). Elevated p-eIF2 $\gamma$  levels were also reflected in a significant (day 7:  $p = 0.0427$  and day 21:  $p = 0.0034$ ) increase in the p-eIF2 $\gamma$ :eIF2 $\gamma$  ratio observed in the brains of flies pan-neuronally expressing GR(1000), compared to controls, which was not seen with other DPRs (Fig. 1a, f, g). Statistical comparison between ages reveals no significant difference in total eIF2 $\gamma$ , p-eIF2 $\gamma$  or p-eIF2 $\gamma$ :eIF2 $\gamma$  ratio between 7 and 21 days for any genotype (Table S1.). Taken together these results demonstrate pan-

neuronal expression of GR(1000) results in a sustained elevation of eIF2 $\gamma$  phosphorylation. Having previously shown motor-dysfunction does not occur until later ages in these flies [49], these observations suggest eIF2 $\gamma$  phosphorylation is an early event, preceding motor dysfunction.

### **Inhibition of the integrated stress response alleviates impaired motor function in *Drosophila* pan-neuronally expressing GR(1000).**

Phosphorylation of eIF2 $\gamma$  is a common and convergent point of the ISR. It is tightly regulated by specific phosphatases and serine/threonine eIF2 $\gamma$  kinases, each of which responds to distinct physiological and pathological stimuli. To explore whether eIF2 $\gamma$  phosphorylation merely correlates with, or is an important mediator of, GR(1000)-induced toxicity we utilised the genetic tractability of *Drosophila* to target specific components of the ISR. We then examined the effect on established phenotypes in flies pan-neuronally expressing GR(1000).

Following the resolution of cellular stress, p-eIF2 $\gamma$  is dephosphorylated by the serine/threonine protein phosphatase 1 (PP1). PP1 is a ubiquitous, promiscuous phosphatase and is directed to dephosphorylate p-eIF2 $\gamma$  by Protein Phosphatase 1 Regulatory Subunit 15A (PPP1R15A). Previous studies have demonstrated that overexpression of the *Drosophila* *PPP1R15A* orthologue, *PPP1R15*, is sufficient to dephosphorylate p-eIF2 $\gamma$  and inhibit the ISR [28]. Having confirmed *PPP1R15* overexpression, which increases *PPP1R15* expression by ~78% (Fig. S1a), significantly ( $p = 0.006$ ) reduced the elevated p-eIF2 $\gamma$ :eIF2 $\gamma$  ratio in flies pan-neuronally expressing GR(1000) (Fig. S1d, e) we observed that pan-neuronal co-expression of *PPP1R15* significantly ( $p = 0.0355$ ) alleviated previously characterised climbing impairments in these flies, compared to those co-expressing GR(1000) with a Gal4 titration control (mCD8-GFP) (Fig. 2a). A titration control is used to control for the effect of driving multiple transgenes under the control of a single Gal4 driver. Climbing assays were performed at 21 days post-eclosion; a timepoint at which we previously showed pan-neuronal expression of GR(1000) caused significant motor impairment [49]. Using activity monitors we also

showed that at 21 days post-eclosion flies pan-neuronally expressing GR(1000) displayed significantly ( $p = 0.0059$ ) fewer movements, in a 24 hour period, than control flies (Fig. 2b), consistent with our previously published data [47]. Critically this reduction in movement was rescued by co-expression of *PPP1R15* (Fig. 2b).

Phosphorylation of mammalian eIF2 $\alpha$  is regulated by four specific serine/threonine eIF2 $\alpha$  kinases, each responding to distinct cellular cues. These kinases are eukaryotic Translation Initiation Factor 2 Alpha Kinases 1,2,3 and 4 (EIF2AK1, EIF2AK2, EIF2AK3 and EIF2AK4), also known as heme-regulated eIF2 $\alpha$  kinase (HRI), Protein Kinase R (PKR), PKR-like endoplasmic reticulum kinase (PERK) and general control nonderepressible 2 (GCN2), respectively. While the core components of the ISR are highly conserved between flies and humans, flies only have two eIF2 $\alpha$  kinases; GCN2 and PERK/PEK. Using previously established RNAi lines, we demonstrated that while pan-neuronal knockdown of *GCN2*, (~16% knockdown (Fig. S1b)), had no significant effect upon climbing ability (Fig. 2c) or activity (Fig. 2d) in control flies, it significantly rescued climbing (Fig. 2c) and activity impairments (Fig. 2d), as well as the elevated p-eIF2 $\alpha$ :eIF2 $\alpha$  ratio (Fig. S1d, e), in GR(1000) flies. Pan-neuronal co-expression of a control RNAi (mCherry-RNAi) with GR(1000) had no effect on either climbing or activity phenotypes (Fig. 2c, d). In contrast to *GCN2*, pan-neuronal knockdown of *PERK/PEK* (~21% knockdown (Fig. S1c)) ameliorated reduced activity, but not climbing defects in GR(1000) flies (Fig. 2c, d). It also only showed a partial rescue of the elevated p-eIF2 $\alpha$ :eIF2 $\alpha$  ratio, showing no significant difference to either controls or GR(1000) expressing flies (Fig. S1). Global knockdown of *PERK/PEK* using an established mutant loss-of-function allele (*PEK<sup>e01744</sup>*), however, was sufficient to reduce both climbing and activity deficits in GR(1000) flies, suggesting that climbing impairments may be underpinned by non-cell autonomous *PERK/PEK* activation by neuronal GR(1000). *PEK<sup>e01744</sup>* also showed a partial rescue of the elevated p-eIF2 $\alpha$ :eIF2 $\alpha$  ratio, showing no significant difference to the control and a notable, albeit not significant ( $p = 0.0675$ ), decrease compared to GR(1000) expressing flies (Fig. S1d, e). Neither pan-neuronal expression of *PEK*-RNAi nor *PEK<sup>e01744</sup>* had any significant effect on climbing or activity in control flies. Taken together this data suggests that inhibition of the ISR at the level of eIF2 $\alpha$  phosphorylation/dephosphorylation can ameliorate toxic phenotypes downstream of

neuronal polyGR. Furthermore, the observation that *GCN2* knockdown or *PPP1R15* overexpression showed a more significant effect on elevated p-eIF2 $\alpha$ :eIF2 $\alpha$  ratio than *PEK* knockdown may suggest that GR(1000) toxicity is driven predominantly through GCN2 dependent activation of the ISR.

### **Arginine-rich DPRs co-localise with and enhance the accumulation of the stress/RNP granules**

Phosphorylation of eIF2 $\alpha$  initiates the formation of stress granules in response to a range of cellular stresses. While stress granules play a protective role, accumulating evidence suggests that chronic stress granule accumulation may contribute towards neurodegeneration in ALS and FTD. Having observed increased eIF2 $\alpha$  phosphorylation and shown that inhibition of the ISR can ameliorate degenerative phenotypes in flies pan-neuronally expressing GR(1000), we asked whether pan-neuronal expression of specific DPR species led to the accumulation of stress granules within neurons. Using the cellular resolution of primary neurons, we showed neuronal cultures from flies pan-neuronally expressing either PR(1000) or GR(1000) demonstrated a significant increase ( $p = 0.031$  and  $p = 0.048$ , respectively) in the percentage of neurons containing puncta positive for the established stress granule marker FMR1, compared to controls (Fig. 3a, b). Anti-HRP was used as an established neuronal marker in *Drosophila* [44, 46], while anti-GFP was used to label GFP-tagged DPRs. Cultures from flies pan-neuronally expressing GA(1000) or AP(1000) showed no significant difference to controls. The percentage of neurons showing FMR1 positive stress granules was even greater when looking specifically at those with visible DPR accumulations (Fig. 3c). In addition to seeing a greater number of neurons with FMR1 positive puncta when PR(1000) or GR(1000) were pan-neuronally expressed, these neurons also showed a significant ( $p < 0.0001$ ) increase in the number of FMR1 positive puncta observed within each neuron (Fig. 3d). The majority of these FMR1 positive puncta were observed to colocalise with PR or GR, and vice versa (Fig. 3e, f). The alternative stress granule marker eukaryotic translation initiation factor 4E (eIF4E) was also observed to accumulate in primary neurons when GR(1000) was pan-neuronally expressed, or when control cells were treated with chemical stressor sodium arsenite (NaAsO<sub>2</sub>) (Fig. S2a, b, c).

A significant increase in the number of FMR1 positive stress granules was also observed *in vivo*, in the brains of 28 day old flies pan-neuronally expressing GR(1000), but not other DPRs, compared to controls (Fig. S2d, e). To explore this further, we examined whether heat stress induced stress granule accumulation, as observed in previous studies and control flies (Fig. S2f, g), could potentiate stress granule formation in flies pan-neuronally expressing GR(1000). Under non-stressed conditions flies pan-neuronally expressing GR(1000) displayed ~ 112 % more FMR1 positive stress granules than GFP expressing controls (Fig. S2d, e). However, following heat stress both GFP controls and GR(1000) expressing flies showed an increase in the number of FMR1 positive puncta (Fig. 4a, b), with GR(1000) flies displaying ~ 194 % more FMR1 positive stress granules than GFP expressing controls. Similarly, following heat stress, flies pan-neuronally expressing GR(1000) displayed ~ 354 % more puncta positive for the stress granule marker ATX2 than GFP expressing controls (Fig. 4c, d). Taken together these results suggest flies pan-neuronally expressing GR(1000) show a greater sensitivity to stress, displaying increased stress granule accumulation under basal and stress conditions, than controls. Additionally, a number of FMR1- and ATX2-positive puncta were observed to co-localize with GR(1000) (Fig. 4a, c). To explore whether this phenotype was conserved in human neurons, we examined C9orf72 repeat expansion patient-derived iPSC motor neurons. Consistent with our findings in *Drosophila*, we observed strong co-localization between ATXN2 and PolyGR in these neurons (Fig. 4e). ATXN2 and PolyGR showed a positive correlation in signal intensity (thresholded Pearson's  $R = 0.63$ ), while thresholded Manders' overlap coefficients demonstrated that 93.9% of the PolyGR signal overlapped with ATXN2 ( $tM2 = 0.939$ ) and 49.1% of the ATXN2 signal overlapped with PolyGR ( $tM1 = 0.491$ ). PolyGR was also observed to co-localize with the stress granule marker G3BP1 (Fig. 4e), showing a strong positive correlation in signal intensity (thresholded Pearson's  $R = 0.85$ ). Furthermore, thresholded Manders' overlap coefficients demonstrated a high degree of co-occurrence between the two proteins, with 94.2% of the PolyGR signal overlapping with G3BP1 ( $tM2 = 0.942$ ) and 82.8% of the G3BP1 signal overlapping with PolyGR ( $tM1 = 0.828$ ). Approximately 20% of neurons in culture presented with visible GR inclusions. These results align with previous proteomic studies demonstrating interactions between PolyGR

and several stress/RNP granule proteins, including G3BP1 and ATXN2 [25]. Furthermore, they confirm the conservation of these pathological phenotypes between *Drosophila* models and human neurons.

**Inhibition of the integrated stress response reduces the number of FMR1 positive puncta observed in *Drosophila* pan-neuronally expressing GR(1000).**

Having shown that Inhibition of the ISR alleviates impaired motor function in *Drosophila* pan-neuronally expressing GR(1000), we asked whether ISR inhibition could also reduce the stress/RNP granule accumulation observed in these flies. Overexpression of PPP1R15, knockdown of GCN2 and knockdown of PEK all significantly reduced the number of FMR1 positive stress/RNP granules observed in the brains of *Drosophila* pan-neuronally expressing GR(1000) at 21 days post-eclosion (Fig. 5).

**Knockdown of ATX2 rescues impaired motor function, seizure phenotypes and stress granule accumulation in *Drosophila* pan-neuronally expressing GR(1000)**

Previous studies have shown that targeted reduction in RNP-/stress-granule formation can convey neuroprotection. *ATXN2*, an established ALS risk gene [14], is essential for normal RNP- and stress-granule formation, mediating their assembly through intrinsically disordered regions (IDRs). Indeed deletion of IDRs in *ATX2* has been shown to reduce toxicity observed when FUS or 50-repeat polyGR are expressed in the *Drosophila* eye [2]. In addition, knockdown of *ATXN2* has previously been shown to be protective in yeast, fly and mouse TDP-43 models of FTD/ALS [3, 14]. Having observed the accumulation of RNP-/stress-granules in GR(1000) expressing flies, we asked whether knockdown of *ATX2* was sufficient to alleviate established phenotypes in these models. Pan-neuronal RNAi-mediated, knockdown of *ATX2* had no significant effect on climbing ability in control, AP(1000), PR(1000) or GA(1000) flies at 28 days post-eclosion (Fig. 6a). However, *ATX2* knockdown significantly ( $p < 0.0001$ ) rescued impaired climbing ability in flies pan-neuronally expressing GR(1000) (Fig. 6a, b). A rescue of impaired climbing ability in flies pan-neuronally expressing GR(1000) was also observed by knockdown of *ATX2* with a

second independent RNAi line (Fig. S3a). Characterisation of knockdown efficiency reveals an ~ 50 % reduction in ATX2 protein levels with both RNAi lines (Fig. S3b, c). Pan-neuronal co-expression of a control RNAi line (mCherry-RNAi) with GR(1000) showed no rescue effect (Fig. S3a). In contrast, over-expression of *ATX2* did not potentiate GR(1000) toxicity and had no significant effect on climbing ability in controls or any DPR expressing line (Fig. 6a, b). Similarly, a modifier screen revealed co-expression of human *ATXN2* carrying either non-pathogenic (22 repeat) or pathogenic (32 repeat) polyglutamine expansions had no effect on the toxicity of any DPR species, when expressed in the *Drosophila* eye (Fig. S3d).

Having shown pan-neuronal knockdown of *ATX2* is sufficient to alleviate impaired climbing ability in flies pan-neuronally expressing GR(1000) we next asked whether *ATX2* knockdown could also rescue the reduced activity observed in these flies. Pan-neuronal expression of GR(1000) with a Gal4 titration control (mCD8-GFP) resulted in a significant ( $p = 0.0073$ ) reduction in the activity of flies observed over a 24 hour period, compared to controls (Fig. 7a, b). Pan-neuronal knockdown of *ATX2* in a GR(1000) background led to a significant ( $p < 0.0001$ ) rescue of reduced activity. In contrast, pan-neuronal knockdown of *ATX2* had no significant effect on the activity of control flies. A control RNAi (mCherry RNAi) had no significant effect on the activity of control or GR(1000) flies.

Previously we found that pan-neuronal co-expression of specific combinations of DPR species induced age-dependent “bang-sensitive” seizure phenotypes. We have subsequently found that subjecting flies to more rigorous mechanical stimulation, by employing an established vortex stimulation assay [30], leads to a significant number of flies pan-neuronally expressing GR(1000) presenting with seizures, at 14 days post-eclosion (Fig. S3e). Pan-neuronal expression of other DPR species did not result in a significant number of seizures being observed (Fig. S3e). We therefore asked whether knockdown of *ATX2* could alleviate seizure phenotypes in flies pan-neuronally expressing GR(1000). At 28 days post-eclosion a significant percentage (~ 58 %,  $p < 0.0001$ ) of flies pan-neuronally expressing GR(1000), with a Gal4 titration control, presented with seizures (Fig. 7c). Pan-neuronal co-expression of *ATX2*-RNAi with GR(1000) resulted in a significant

reduction ( $\sim 27\%$ ,  $p = 0.0128$ ) in the number of flies exhibiting seizures and significantly ( $p = 0.0078$ ) decreased seizure duration (Fig. 7d).

Having shown that knockdown of *ATX2* was sufficient to ameliorate climbing deficits, reduced activity and seizure phenotypes in *Drosophila* pan-neuronally expressing GR(1000), we looked to determine whether *ATX2* knockdown could also reduce the stress/RNP granule accumulation phenotype observed in GR(1000) flies, or whether the rescue of motor and seizure phenotypes was independent of this. Knockdown of *ATX2* in controls had no effect on the mean number of FMR1-positive puncta per neuron or the number of neurons containing FMR1-positive stress/RNP granules per GFP positive neuron (Fig. 8a, b, c). In contrast, *ATX2* knockdown in GR(1000) expressing neurons led to a significant reduction in both the number of FMR1-positive puncta per neuron (Fig. 8a, b,  $p = 0.0002$ ) and the percentage of neurons with GR inclusions containing FMR1-positive stress/RNP granules (Fig. 8a-c). *ATX2* knockdown also significantly ( $p = 0.0025$ ) reduced the increased p-eIF2 $\alpha$ /eIF2 $\alpha$  ratio observed in flies pan-neuronally expressing GR(1000) (Fig. S1d, e), suggesting that despite *ATX2* dependent stress granule formation being downstream of eIF2 $\alpha$  phosphorylation, and the ISR, persistent accumulation of stress granules may potentiate ISR activation.

### **Knockdown of *ATXN2* ameliorates perturbations to neuronal morphology in mouse primary neurons transduced with PolyGR**

Alterations to neuronal morphology, including the reduced complexity of dendritic arborisation has been observed in C9orf72 and DPR models [17, 22]. In our preliminary studies we observed an apparent reduction in dendritic complexity in mouse primary neurons transduced with either 100 or 200 repeats of PolyGR. We therefore looked to determine whether knockdown of *ATXN2* was sufficient to alleviate reduced dendritic complexity in these models. Transduction of GR(100) with a control shRNA caused a

significant reduction in dendritic complexity when compared to cells transduced with a control shRNA alone ( $p = 0.0144$ ) or co-transduced with GFP and the control shRNA ( $p = 0.0183$ ) (Fig. 9a, b). Reduced complexity was also observed when neurons were co-transduced with GR(200) and the control shRNA ( $p = 0.0152$  vs control shRNA and  $p = 0.0193$  vs GFP + control shRNA) (Fig. 9a, b). Co-transduction of GR(100) with an ATXN2 shRNA resulted in a partial, albeit non-significant ( $p = 0.0581$ ), rescue of this phenotype, whilst co-transduction of GR(200) with an ATXN2 shRNA resulted in a significant ( $p = 0.0235$ ) partial rescue (Fig. 9a, b). These findings highlight a conserved role for ATXN2 knockdown in conveying neuroprotection in both *Drosophila* and mammalian models.

## Discussion

In this study we demonstrate that neuronal GR(1000) leads to a significant increase in the phosphorylation of eIF2 $\alpha$ , the core of the ISR, as well as accumulation of stress granule markers, FMR1 and ATX2, in the brains of *Drosophila*. In addition, we find stress granule markers colocalise with GR aggregates in *Drosophila* brains, primary neurons and patient-derived motor neurons. These findings suggest that activation of the ISR and accumulation of stress granules, two intrinsically linked pathways previously implicated in C9orf72-related FTD/ALS, may be driven by polyGR. Critically, we demonstrate that genetic inhibition of the ISR or ATXN2, a key regulator of stress granules, can alleviate previously established phenotypes, including impaired motor function and activity deficits, in *Drosophila* pan-neuronally expressing GR(1000). Supporting this we show knockdown of ATXN2 to be protective in mouse primary neurons transduced with GR(200). Taken together these observations demonstrate the role of stress granules and the wider ISR in the pathophysiology of C9orf72-related FTD/ALS and reveal ATXN2 and the ISR to be promising targets for potential treatment of C9orf72-related FTD/ALS, and perhaps FTD/ALS spectrum disorders more broadly.

Converging lines of evidence indicate that both the ISR and dysregulated stress granule dynamics contribute to the pathogenesis of ALS and FTD [10, 15, 18, 20, 33, 40, 50, 51]. These pathways are intrinsically linked with phosphorylation of the central ISR component

eIF2 $\alpha$ , triggering stress granule formation [33]. Elevated levels of p-eIF2 $\alpha$  and stress granule accumulation have previously been demonstrated in both C9orf72 patient-derived cell models and patient tissue, however the mechanisms leading to this and whether it is underpinned by specific DPR species remains unclear [18, 20, 33, 40, 50, 51]. eIF2 $\alpha$  phosphorylation and ISR activation have been shown to enhance RAN translation and DPR production, whilst the G<sub>4</sub>C<sub>2</sub> repeat expansion, in turn, promotes ISR activation, creating a potential toxic feed forward mechanism [10, 15, 33]. Indeed, whilst both the ISR and stress granules are essential for normal cellular function, maintaining cellular homeostasis in response to various cellular stressors, there is increasing evidence to show that chronic activation of the ISR and/or aberrant, prolonged persistence of stress granules can lead to neurotoxicity and neurodegeneration. Accumulation of stress granules may occur either due to a failure to clear stress granules or from chronic ISR activation promoting stress granule formation. In this study the observation that levels of p-eIF2 $\alpha$  are elevated in the brains of flies expressing GR(1000), but not those expressing other DPRs, prior to the onset of motor phenotypes suggests ISR activation by polyGR may be an early pathogenic event leading to chronic activation of the ISR, aberrant accumulation of stress granules and downstream toxicity. Whilst, in contrast to GR(1000), we did not observe elevated p-eIF2 $\alpha$  in the brains of flies pan-neuronally expressing PR(1000), a previous study from Kramer et al., (2018) showed transcriptional upregulation of genes involved in endoplasmic reticulum stress and the ISR in both mouse primary neurons transduced with PR(50), and K562 cells, a human immortalized lymphoblast cell line, treated with synthetic PR(20) [24]. They also found pre-treatment of PR(20) treated K562 cells with the ISR inhibitor ISRIB improved viability of these cells [24]. This disparity in which DPRs trigger the ISR and downstream toxicity may be attributed to differences in the capacity of *in vitro* and *in vivo* systems to mediate cellular stress responses and/or the levels of exogenous stress these systems are exposed to in an experimental setting. Supporting this we show that despite p-eIF2 $\alpha$  levels not being elevated in PR(1000) fly brains, we did observe accumulation of stress granules in primary neurons cultured from these flies.

Critically, supporting the ISR as a potential therapeutic target, our genetic dissection suggests the ISR can be targeted at various points, including knockdown of eIF2 $\alpha$  kinases *GCN2* or *PEK*, or upregulation of the eIF2 $\alpha$  phosphatase *PPP1R15*, to ameliorate motor dysfunction in GR(1000) expressing flies. Taken together these observations support the hypothesis that chronic activation of the ISR leads to neurodegeneration, with ISR inhibition offering an attractive therapeutic target. This is supported by similar observations in other pre-clinical FTD/ALS models. For example, previous studies have shown that the PERK inhibitor GSK2606414 was sufficient to mitigate TDP-43 toxicity in both *Drosophila* and rat primary cortical neurons [23]. Similarly, studies have demonstrated that inhibition of either GCN2 or PERK, or inhibition of the ISR using ISRIB can convey neuroprotection in mouse models of Alzheimer's disease [27, 32], whilst GSK2606414 was protective in mouse models of Parkinson's disease [29]. ISR inhibitors such as ISRIB have also been shown to block eIF2 $\alpha$  phosphorylation-induced stress granule formation [43]. Collectively these findings highlight the potential for small molecule ISR inhibitors such as ISRIB for the treatment of FTD/ALS spectrum disorders.

In addition to showing that ISR inhibition prevented toxicity in GR(1000) flies we found that knockdown of the stress granule regulator ATX2/ATXN2 was sufficient to mitigate toxicity in both GR(1000) flies and mouse primary neurons transduced with PolyGR. ATXN2 is an RNA binding protein that plays a fundamental role in mRNA translation, RNA regulation, the assembly of processing bodies (P-bodies) and the formation of stress granules. Polyglutamine expansions with the *ATXN2* gene have been implicated in several neurodegenerative diseases, including spinocerebellar ataxia type 2 (SCA2) [19, 39], ALS and FTD [14, 37]. In healthy individuals the *ATXN2* polyglutamine tract typically comprises 22-23 glutamine residues (polyQs). In SCA2 this is expanded to >35 repeats, with intermediate expansions (24-34 repeats) conferring increased ALS risk. Intermediate expansions have also been detected with higher frequency in bvFTD cases [37]. Previous studies have suggested that intermediate expansions may reduce the clearance of ATXN2, leading to elevated levels and downstream toxicity [14]. However, in this study pan-neuronal overexpression of ATX2 had no effect on established phenotypes observed in our

DPR fly models. In addition, expression of human ATXN2 with normal (22Q) and intermediate (32Q) polyglutamine expansions did not modify DPR toxicity, when expressed in the *Drosophila* eye. Flies pan-neuronally expressing GR(1000) also did not show elevated levels of ATX2, suggesting toxicity in these flies is not driven by increased ATX2. In contrast, knockdown of *ATX2* was sufficient to alleviate all phenotypes characterised in the GR(1000) fly model, as well as mouse primary neurons transduced with PolyGR, highlighting *ATX2* knockdown as a potential therapeutic target in ALS/FTD. Indeed, previous studies have shown *ATX2/ATXN2* knockdown to be protective in several TDP-43 models of ALS, including *Drosophila*, yeast, and mice [3, 14]. For example, Becker et al., (2017) demonstrated that knockdown of *ATXN2* in TDP-43 transgenic mice, using small interfering RNAs (siRNAs) or antisense-oligonucleotides (ASO), reduced TDP-43 toxicity by decreasing its transit to, and propensity to aggregate within, stress granules [3]. This resulted in a dose dependent slowing of disease progression, improved motor function and increased survival. This study was key in establishing ATXN2 as a therapeutic target for ALS, and implicating stress granules in the pathophysiology of the disease. The results of preclinical studies targeting *ATXN2* in TDP-43 models has underpinned *ATXN2* as an attractive target for potential therapeutic intervention. Now we show this may also be the case for C9orf72 related FTD/ALS. While a recent clinical trial (NCT04494256) assessing the effectiveness of ATXN2 ASOs for ALS proved unsuccessful, the effectiveness of this approach in pre-clinical models suggests targeting *ATXN2* much earlier may be critical for effective intervention. Indeed, the findings of our study demonstrate that activation of the ISR occurs as an early event, preceding motor and behavioural dysfunction, in *Drosophila* pan-neuronally expressing GR(1000). In addition, while ATXN2 ASOs were shown to effectively reduce ATXN2 levels in cerebral spinal fluid, their ability to reach and sustain therapeutic levels in affected motor neurons may have been insufficient. Further studies will be critical to assess whether earlier intervention, improved delivery, or complementary strategies such as targeting both the ISR and ATXN2 simultaneously, could enhance effectiveness in a clinical setting.

Utilising the genetic tractability of *Drosophila* models, expressing DPRs of a length comparable to the longest repeats observed in C9orf72 patients, this study demonstrates that neuronal PolyGR activates the ISR and promotes stress granule accumulation. These two intrinsically linked pathways have both been implicated in the pathogenesis of ALS and FTD. Thus, our findings demonstrating genetic inhibition of the ISR or ATXN2 conveys neuroprotection underscores these pathways as important therapeutic targets for C9orf72-related FTD/ALS, and possibly other FTD/ALS spectrum disorders.

### **Declarations**

#### **Ethics approval and consent to participate**

not applicable

#### **Consent to Publish declaration**

not applicable

#### **Availability of Data and Materials**

The datasets used and/or analysed during the current study available from the corresponding author on reasonable request.

#### **Competing interests**

The authors declare that they have no competing interests

#### **Funding**

NSH was supported by funding from the Jean Corsan Foundation, ARL was supported by NIH R35 NS122140. RJHW was supported by Alzheimer's Society grants (510 and 611). JS was supported Alzheimer's Society grant 630 and The Heather Corrie Impact Fund. MSA was supported by a MND association Ph.D. Studentship (Livesey/Oct20/900-792). Stocks obtained from the Bloomington *Drosophila* Stock Center (NIH P40OD018537) were used in this study. Work on this project benefited from the Manchester Fly Facility, established through funds from the University and the Wellcome Trust (087742/Z/08/Z).'

#### **Author Contributions**

NSH contributed to the conception of the project, developed the methodology, validated results, performed formal analysis and investigation, curated the data, created visualizations, and wrote the original draft. JLS contributed to investigation and formal analysis, and reviewed and edited the manuscript. JS contributed to investigation and formal analysis, and reviewed and edited the manuscript. RG contributed to the investigation. JXC performed formal analysis. SPA contributed to formal analysis and reviewed, and edited, the manuscript. MSA contributed to the investigation. SPB contributed to the conceptualization of the study and secured funding. MRL contributed to conceptualization and methodology, provided resources, supervised the work, and reviewed and edited the manuscript. CLB contributed to conceptualization and supervision, performed formal analysis, and reviewed and edited the manuscript. AP contributed to conceptualization and methodology, provided resources, supervised the study, secured funding, performed formal analysis, and reviewed and edited the manuscript. ARLS contributed to conceptualization and methodology, secured funding, performed formal analysis, and reviewed and edited the manuscript. RJHW conceived and designed the study, validated and analyzed the data, carried out investigation and data curation, wrote the original draft, created visualizations, supervised the project, managed project administration, and secured funding. All authors read and approved the final manuscript.

### **Acknowledgements**

We gratefully acknowledge Sebastian Michels and Kevin Sanchez for their invaluable assistance with early pilot studies, which laid a foundation for the PCN study. We thank Professor Leonard Petrucelli (Mayo Clinic, Jacksonville, FL) for kindly donating C9-AAV DPR vectors for this study. We thank Prof. Mani Ramaswami (Trinity College, Dublin) for his kind gift of the ATX2 antibody.

### **References**

- 1 Aragon-Gonzalez A, Shaw AC, Kok JR, Roussel FS, Santos Souza CD, Granger SM, Vetter T, de Diego Y, Meyer KC, Beal SNet al (2024) C9ORF72 patient-derived endothelial cells drive blood-brain barrier disruption and

- contribute to neurotoxicity. *Fluids Barriers CNS* 21: 34 Doi 10.1186/s12987-024-00528-6
- 2 Bakthavachalu B, Huelsmeier J, Sudhakaran IP, Hillebrand J, Singh A, Petrauskas A, Thiagarajan D, Sankaranarayanan M, Mizoue L, Anderson EN et al (2018) RNP-Granule Assembly via Ataxin-2 Disordered Domains Is Required for Long-Term Memory and Neurodegeneration. *Neuron* 98: 754-766.e754 Doi 10.1016/j.neuron.2018.04.032
  - 3 Becker LA, Huang B, Bieri G, Ma R, Knowles DA, Jafar-Nejad P, Messing J, Kim HJ, Soriano A, Auburger Get al (2017) Therapeutic reduction of ataxin-2 extends lifespan and reduces pathology in TDP-43 mice. *Nature* 544: 367-371 Doi 10.1038/nature22038
  - 4 Bennett CL, Dastidar S, Arnold FJ, McKinstry SU, Stockford C, Freibaum BD, Sopher BL, Wu M, Seidner G, Joiner Wet al (2023) Senataxin helicase, the causal gene defect in ALS4, is a significant modifier of C9orf72 ALS G4C2 and arginine-containing dipeptide repeat toxicity. *Acta Neuropathol Commun* 11: 164 Doi 10.1186/s40478-023-01665-z
  - 5 Bennion Callister J, Ryan S, Sim J, Rollinson S, Pickering-Brown SM (2016) Modelling C9orf72 dipeptide repeat proteins of a physiologically relevant size. *Human Molecular Genetics* 25: 5069-5082 Doi 10.1093/hmg/ddw327
  - 6 Bischof J, Bjorklund M, Furger E, Schertel C, Taipale J, Basler K (2013) A versatile platform for creating a comprehensive UAS-ORFeome library in *Drosophila*. *Development* 140: 2434-2442 Doi 10.1242/dev.088757
  - 7 Boeynaems S, Bogaert E, Kovacs D, Konijnenberg A, Timmerman E, Volkov A, Guharoy M, De Decker M, Jaspers T, Ryan VHet al (2017) Phase Separation of C9orf72 Dipeptide Repeats Perturbs Stress Granule Dynamics. *Mol Cell* 65: 1044-1055.e1045 Doi 10.1016/j.molcel.2017.02.013

- 8 Bond S, Lopez-Lloreda C, Gannon PJ, Akay-Espinoza C, Jordan-Sciutto KL (2020) The Integrated Stress Response and Phosphorylated Eukaryotic Initiation Factor 2alpha in Neurodegeneration. *J Neuropathol Exp Neurol* 79: 123-143 Doi 10.1093/jnen/nlz129
- 9 Castelli LM, Cutillo L, Souza CDS, Sanchez-Martinez A, Granata I, Lin YH, Myszczyńska MA, Heath PR, Livesey MR, Ning Ket al (2021) SRSF1-dependent inhibition of C9ORF72-repeat RNA nuclear export: genome-wide mechanisms for neuroprotection in amyotrophic lateral sclerosis. *Mol Neurodegener* 16: 53 Doi 10.1186/s13024-021-00475-y
- 10 Cheng W, Wang S, Mestre A, Fu C, Makarem A, Xian F, Hayes L, Lopez-Gonzalez R, Drenner K, Jiang Jet al (2018) C9ORF72 GGGGCC repeat-associated non-AUG translation is upregulated by stress through eIF2 $\alpha$  phosphorylation. *Nature communications* 9: 51 Doi 10.1038/s41467-017-02495-z
- 11 Chew J, Cook C, Gendron TF, Jansen-West K, Del Rosso G, Daugherty LM, Castanedes-Casey M, Kurti A, Stankowski JN, Disney MD (2019) Aberrant deposition of stress granule-resident proteins linked to C9orf72-associated TDP-43 proteinopathy. *Molecular neurodegeneration* 14: 1-15
- 12 DeJesus-Hernandez M, Mackenzie IR, Boeve BF, Boxer AL, Baker M, Rutherford NJ, Nicholson AM, Finch NA, Flynn H, Adamson Jet al (2011) Expanded GGGGCC hexanucleotide repeat in noncoding region of C9ORF72 causes chromosome 9p-linked FTD and ALS. *Neuron* 72: 245-256 Doi 10.1016/j.neuron.2011.09.011
- 13 Du ZW, Chen H, Liu H, Lu J, Qian K, Huang CL, Zhong X, Fan F, Zhang SC (2015) Generation and expansion of highly pure motor neuron progenitors from human pluripotent stem cells. *Nat Commun* 6: 6626 Doi 10.1038/ncomms7626

- 14 Elden AC, Kim HJ, Hart MP, Chen-Plotkin AS, Johnson BS, Fang X, Armakola M, Geser F, Greene R, Lu MM et al (2010) Ataxin-2 intermediate-length polyglutamine expansions are associated with increased risk for ALS. *Nature* 466: 1069-1075 Doi 10.1038/nature09320
- 15 Green K, Glineburg M, Kearse M, Flores B, Linsalata A, Fedak S, Goldstrohm A, Barmada S, Todd P (2017) RAN translation at C9orf72-associated repeat expansions is selectively enhanced by the integrated stress response. *Nature communications* 8: 2005 Doi 10.1038/s41467-017-02200-0
- 16 Green KM, Glineburg MR, Kearse MG, Flores BN, Linsalata AE, Fedak SJ, Goldstrohm AC, Barmada SJ, Todd PK (2017) RAN translation at C9orf72-associated repeat expansions is selectively enhanced by the integrated stress response. *Nature Communications* 8: Doi 10.1038/s41467-017-02200-0
- 17 Ho WY, Tai YK, Chang JC, Liang J, Tyan SH, Chen S, Guan JL, Zhou H, Shen HM, Koo E et al (2019) The ALS-FTD-linked gene product, C9orf72, regulates neuronal morphogenesis via autophagy. *Autophagy* 15: 827-842 Doi 10.1080/15548627.2019.1569441
- 18 Ilieva E, Ayala V, Jové M, Dalfo E, Cacabelos D, Povedano M, Bellmunt M, Ferrer I, Pamplona R, Portero-Otín M (2007) Oxidative and endoplasmic reticulum stress interplay in sporadic amyotrophic lateral sclerosis. *Brain : a journal of neurology* 130: 3111-3123 Doi 10.1093/brain/awm190
- 19 Imbert G, Saudou F, Yvert G, Devys D, Trottier Y, Garnier JM, Weber C, Mandel JL, Cancel G, Abbas N et al (1996) Cloning of the gene for spinocerebellar ataxia 2 reveals a locus with high sensitivity to expanded CAG/glutamine repeats. *Nat Genet* 14: 285-291 Doi 10.1038/ng1196-285

- 20 Ito Y, Yamada M, Tanaka H, Aida K, Tsuruma K, Shimazawa M, Hozumi I, Inuzuka T, Takahashi H, Hara H (2009) Involvement of CHOP, an ER-stress apoptotic mediator, in both human sporadic ALS and ALS model mice. *Neurobiology of disease* 36: 470-476 Doi 10.1016/j.nbd.2009.08.013
- 21 Jafarinia H, van der Giessen E, Onck P (2020) Phase Separation of Toxic Dipeptide Repeat Proteins Related to C9orf72 ALS/FTD. *Biophysical journal* 119: 843-851 Doi 10.1016/j.bpj.2020.07.005
- 22 Kaliszewska A, Allison J, Col TT, Shaw C, Arias N (2022) Elucidating the Role of Cerebellar Synaptic Dysfunction in C9orf72-ALS/FTD - a Systematic Review and Meta-Analysis. *Cerebellum* 21: 681-714 Doi 10.1007/s12311-021-01320-0
- 23 Kim HJ, Raphael AR, LaDow ES, McGurk L, Weber RA, Trojanowski JQ, Lee VM, Finkbeiner S, Gitler AD, Bonini NM (2014) Therapeutic modulation of eIF2alpha phosphorylation rescues TDP-43 toxicity in amyotrophic lateral sclerosis disease models. *Nat Genet* 46: 152-160 Doi 10.1038/ng.2853
- 24 Kramer NJ, Haney MS, Morgens DW, Jovicic A, Couthouis J, Li A, Ousey J, Ma R, Bieri G, Tsui CK et al (2018) CRISPR-Cas9 screens in human cells and primary neurons identify modifiers of C9ORF72 dipeptide-repeat-protein toxicity. *Nat Genet* 50: 603-612 Doi 10.1038/s41588-018-0070-7
- 25 Lee KH, Zhang P, Kim HJ, Mitrea DM, Sarkar M, Freibaum BD, Cika J, Coughlin M, Messing J, Molliex A et al (2016) C9orf72 Dipeptide Repeats Impair the Assembly, Dynamics, and Function of Membrane-Less Organelles. *Cell* 167: 774-788 e717 Doi 10.1016/j.cell.2016.10.002
- 26 Lee KH, Zhang P, Kim HJ, Mitrea DM, Sarkar M, Freibaum BD, Cika J, Coughlin M, Messing J, Molliex A et al (2016) C9orf72 Dipeptide Repeats Impair the Assembly, Dynamics, and Function of Membrane-Less Organelles. *Cell* 167: 774-788.e717 Doi 10.1016/j.cell.2016.10.002

- 27 Ma T, Trinh MA, Wexler AJ, Bourbon C, Gatti E, Pierre P, Cavener DR, Klann E (2013) Suppression of eIF2alpha kinases alleviates Alzheimer's disease-related plasticity and memory deficits. *Nat Neurosci* 16: 1299-1305 Doi 10.1038/nn.3486
- 28 Malzer E, Szajewska-Skuta M, Dalton LE, Thomas SE, Hu N, Skaer H, Lomas DA, Crowther DC, Marciniak SJ (2013) Coordinate regulation of eIF2alpha phosphorylation by PPP1R15 and GCN2 is required during *Drosophila* development. *J Cell Sci* 126: 1406-1415 Doi 10.1242/jcs.117614
- 29 Mercado G, Castillo V, Soto P, Lopez N, Axten JM, Sardi SP, Hoozemans JJM, Hetz C (2018) Targeting PERK signaling with the small molecule GSK2606414 prevents neurodegeneration in a model of Parkinson's disease. *Neurobiol Dis* 112: 136-148 Doi 10.1016/j.nbd.2018.01.004
- 30 Mituzaitė J, Petersen R, Claridge-Chang A, Baines RA (2021) Characterization of Seizure Induction Methods in *Drosophila*. *eNeuro* 8: Doi 10.1523/ENEURO.0079-21.2021
- 31 Mizielinska S, Gronke S, Niccoli T, Ridler CE, Clayton EL, Devoy A, Moens T, Norona FE, Woollacott IOC, Pietrzyk J et al (2014) C9orf72 repeat expansions cause neurodegeneration in *Drosophila* through arginine-rich proteins. *Science* 345: 1192-1194 Doi 10.1126/science.1256800
- 32 Oliveira MM, Lourenco MV, Longo F, Kasica NP, Yang W, Ureta G, Ferreira DDP, Mendonca PHJ, Bernales S, Ma Tet et al (2021) Correction of eIF2-dependent defects in brain protein synthesis, synaptic plasticity, and memory in mouse models of Alzheimer's disease. *Sci Signal* 14: Doi 10.1126/scisignal.abc5429
- 33 Parameswaran J, Zhang N, Braems E, Tilahun K, Pant D, Yin K, Asress S, Heeren K, Banerjee A, Davis E et al (2023) Antisense, but not sense, repeat

- expanded RNAs activate PKR/eIF2 $\alpha$ -dependent ISR in C9ORF72 FTD/ALS.  
eLife 12: e85902 Doi 10.7554/eLife.85902
- 34 Qu Y, Hahn I, Lees M, Parkin J, Voelzmann A, Dorey K, Rathbone A, Friel CT, Allan VJ, Okenve-Ramos Pet al (2019) Efa6 protects axons and regulates their growth and branching by inhibiting microtubule polymerisation at the cortex. *Elife* 8: Doi 10.7554/eLife.50319
- 35 Qu Y, Hahn I, Webb SE, Pearce SP, Prokop A (2017) Periodic actin structures in neuronal axons are required to maintain microtubules. *Mol Biol Cell* 28: 296-308 Doi 10.1091/mbc.E16-10-0727
- 36 Renton AE, Majounie E, Waite A, Simon-Sanchez J, Rollinson S, Gibbs JR, Schymick JC, Laaksovirta H, van Swieten JC, Myllykangas Let al (2011) A hexanucleotide repeat expansion in C9ORF72 is the cause of chromosome 9p21-linked ALS-FTD. *Neuron* 72: 257-268 Doi 10.1016/j.neuron.2011.09.010
- 37 Rosas I, Martinez C, Clarimon J, Lleó A, Illan-Gala I, Dols-Icardo O, Borroni B, Almeida MR, van der Zee J, Van Broeckhoven Cet al (2020) Role for ATXN1, ATXN2, and HTT intermediate repeats in frontotemporal dementia and Alzheimer's disease. *Neurobiol Aging* 87: 139 e131-139 e137 Doi 10.1016/j.neurobiolaging.2019.10.017
- 38 Sanchez-Soriano N, Goncalves-Pimentel C, Beaven R, Haessler U, Ofner-Ziegenfuss L, Ballestrem C, Prokop A (2010) *Drosophila* growth cones: a genetically tractable platform for the analysis of axonal growth dynamics. *Dev Neurobiol* 70: 58-71 Doi 10.1002/dneu.20762
- 39 Sanpei K, Takano H, Igarashi S, Sato T, Oyake M, Sasaki H, Wakisaka A, Tashiro K, Ishida Y, Ikeuchi Tet al (1996) Identification of the spinocerebellar ataxia type 2 gene using a direct identification of repeat

- expansion and cloning technique, DIRECT. Nat Genet 14: 277-284 Doi 10.1038/ng1196-277
- 40 Sasaki S (2010) Endoplasmic Reticulum Stress in Motor Neurons of the Spinal Cord in Sporadic Amyotrophic Lateral Sclerosis. Journal of Neuropathology & Experimental Neurology 69: 346-355 Doi 10.1097/NEN.0b013e3181d44992
- 41 Schindelin J, Arganda-Carreras I, Frise E, Kaynig V, Longair M, Pietzsch T, Preibisch S, Rueden C, Saalfeld S, Schmid B (2012) Fiji: an open-source platform for biological-image analysis. Nature methods 9: 676-682
- 42 Sharpe JL, Harper NS, West RJH (2022) Identification and Monitoring of Nucleotide Repeat Expansions Using Southern Blotting in Drosophila Models of C9orf72 Motor Neuron Disease and Frontotemporal Dementia. Bio Protoc 12: e4424 Doi 10.21769/BioProtoc.4424
- 43 Sidrauski C, McGeachy AM, Ingolia NT, Walter P (2015) The small molecule ISRIB reverses the effects of eIF2alpha phosphorylation on translation and stress granule assembly. Elife 4: Doi 10.7554/eLife.05033
- 44 Sun B, Salvaterra PM (1995) Characterization of nervana, a Drosophila melanogaster neuron-specific glycoprotein antigen recognized by anti-horseradish peroxidase antibodies. J Neurochem 65: 434-443 Doi 10.1046/j.1471-4159.1995.65010434.x
- 45 Van Nerom M, Ahmed J, Lazar T, Van Lindt J, Panca R, Maes D, Tompa P (2024) C9orf72-linked arginine-rich dipeptide repeats aggravate pathological phase separation of G3BP1. Proc Natl Acad Sci U S A 121 (50) e2402847121: Doi 10.1073/pnas.2402847121
- 46 Wang X, Sun B, Yasuyama K, Salvaterra PM (1994) Biochemical analysis of proteins recognized by anti-HRP antibodies in Drosophila melanogaster: identification and characterization of neuron specific and male specific

- glycoproteins. *Insect Biochem Mol Biol* 24: 233-242 Doi 10.1016/0965-1748(94)90002-7
- 47 Webster CP, Hall B, Crossley OM, Dauletalina D, King M, Lin YH, Castelli LM, Yang ZL, Coldicott I, Kyrgiou-Balli E et al (2025) RuvBL1/2 reduce toxic dipeptide repeat protein burden in multiple models of C9orf72-ALS/FTD. *Life Sci Alliance* 8: Doi 10.26508/lsa.202402757
- 48 Webster CP, Smith EF, Bauer CS, Moller A, Hautbergue GM, Ferraiuolo L, Myszczyńska MA, Higginbottom A, Walsh MJ, Whitworth AJ et al (2016) The C9orf72 protein interacts with Rab1a and the ULK1 complex to regulate initiation of autophagy. *The EMBO Journal* 35: 1656-1676 Doi 10.15252/emj.201694401
- 49 West RJH, Sharpe JL, Voelzmann A, Munro AL, Hahn I, Baines RA, Pickering-Brown S (2020) Co-expression of C9orf72 related dipeptide-repeats over 1000 repeat units reveals age- and combination-specific phenotypic profiles in *Drosophila*. *Acta Neuropathologica Communications* 8: 1-19 Doi doi:10.1186/s40478-020-01028-y
- 50 Zhang K, Daigle JG, Cunningham KM, Coyne AN, Ruan K, Grima JC, Bowen KE, Wadhwa H, Yang P, Rigo F et al (2018) Stress granule assembly disrupts nucleocytoplasmic transport. *Cell* 173: 958-971 e917 Doi 10.1016/j.cell.2018.03.025
- 51 Zhang YJ, Gendron TF, Ebbert MTW, O'Raw AD, Yue M, Jansen-West K, Zhang X, Prudencio M, Chew J, Cook CNet et al (2018) Poly(GR) impairs protein translation and stress granule dynamics in C9orf72-associated frontotemporal dementia and amyotrophic lateral sclerosis. *Nat Med* 24: 1136-1142 Doi 10.1038/s41591-018-0071-1

ARTICLE IN PRESS

## Figures

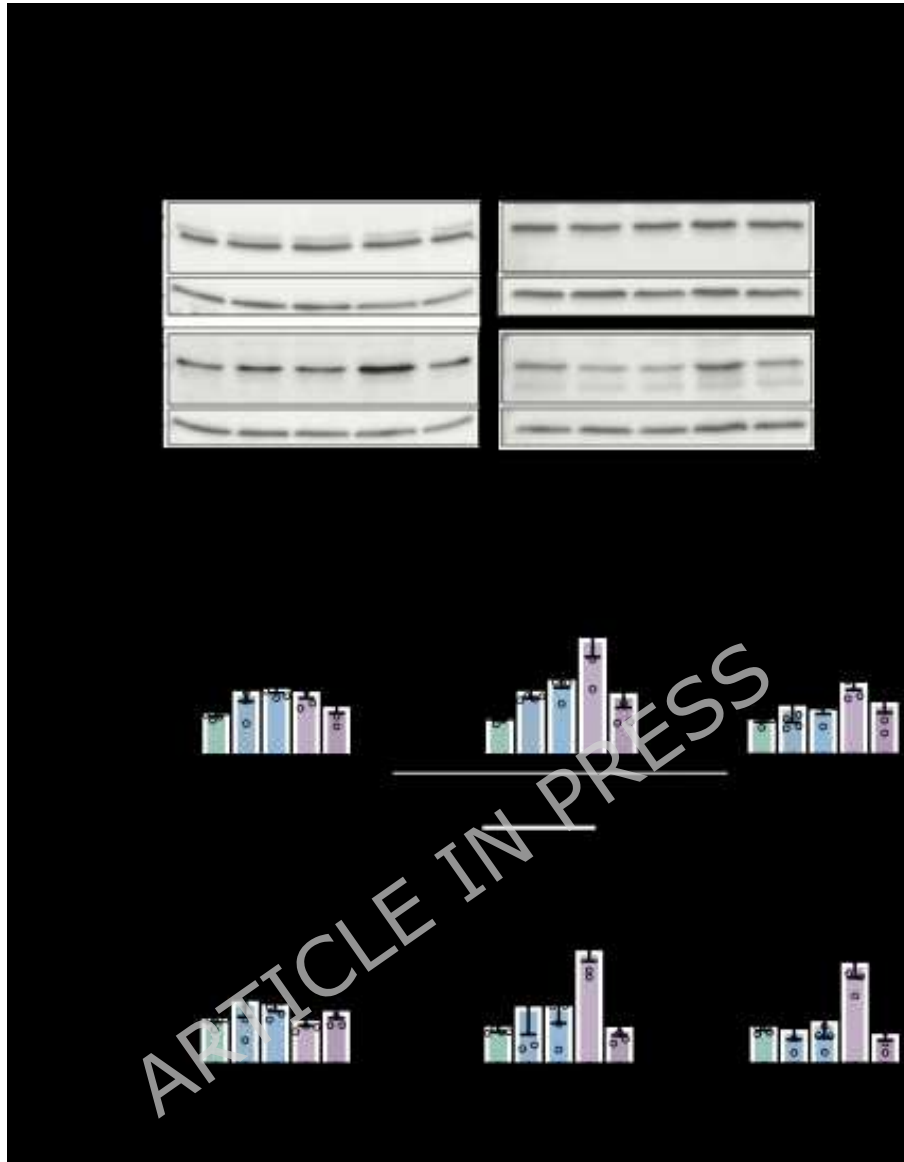


**Fig. 1. Pan-neuronal Expression of GR(1000) Increases eIF2 $\alpha$  phosphorylation in *Drosophila* Heads**

**a.** Representative western blots showing elevated levels of p-eIF2 $\alpha$  in the heads of *Drosophila* pan-neuronally (nSyb-Gal4) expressing 1000-repeat DPRs, or an mCD8-GFP control.

**b-g.** Quantification of the relative abundance of eIF2 $\alpha$  (**b,c**), p-eIF2 $\alpha$  (**d,e**) and the p-eIF2 $\alpha$ /eIF2 $\alpha$  ratio (**f,g**) in the heads of flies pan-neuronally expressing 1000-repeat DPRs, or an mCD8-GFP control at 7 and 21 days post-eclosion. Error bars = SEM, ANOVA with post-hoc Dunnett's comparison to controls \*  $p < 0.05$ , \*\*  $p < 0.01$ , \*\*\*  $p < 0.001$ .

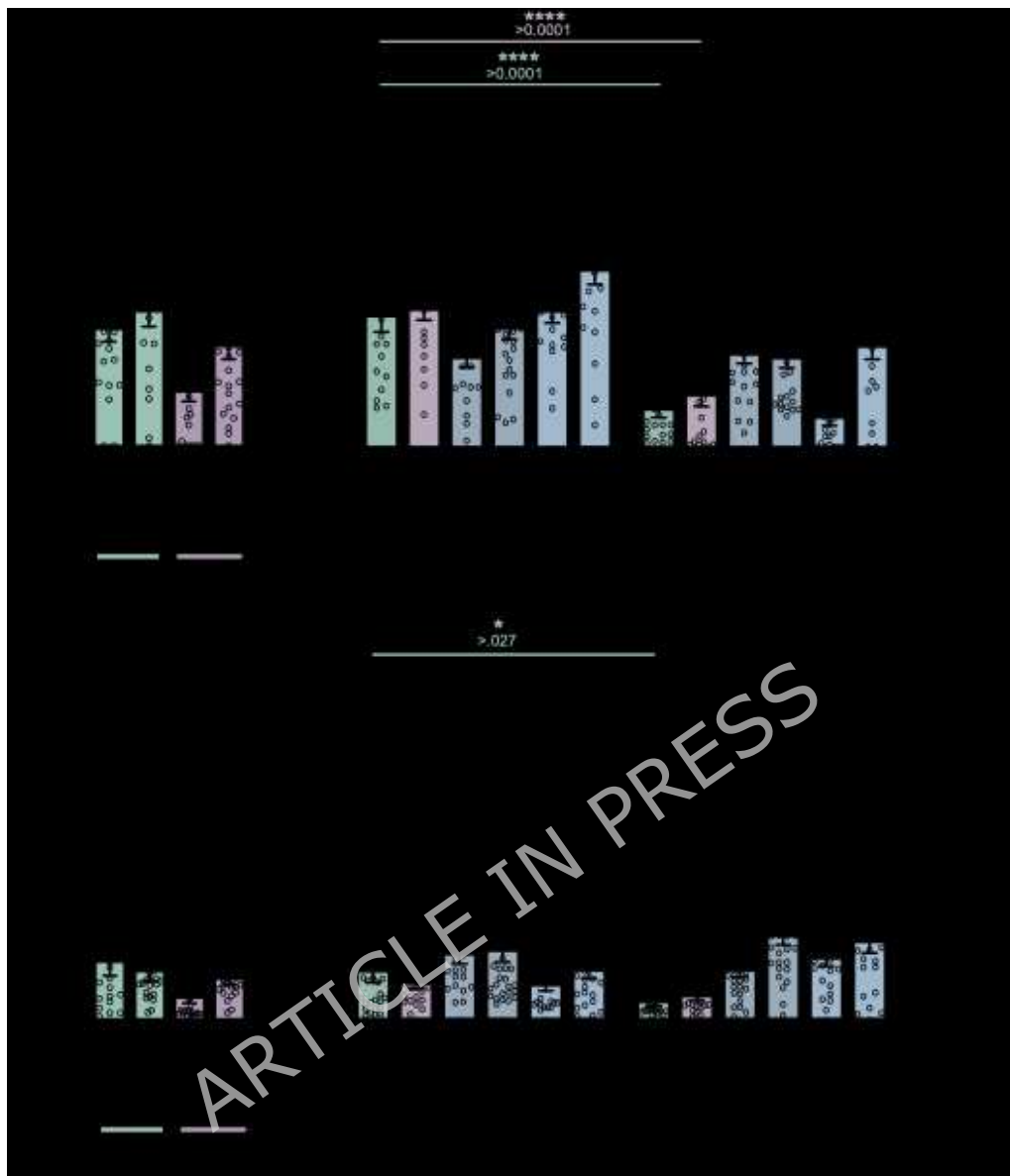


**Fig. 2. Inhibition of the Integrated Stress Response Alleviates Motor and Activity Deficits in *Drosophila* GR(1000) Models**

**a-b.** Overexpression of the eIF2 $\gamma$  phosphatase PPP1R15 rescues impaired climbing (**a**) and activity (**b**) phenotypes in *Drosophila* pan-neuronally (nSyb-Gal4) expressing GR(1000) at 21 days post-eclosion. Error bars = SEM, Kruskal-Wallis with post-hoc Dunn's comparison to controls \*  $p < 0.05$ , \*\*  $p < 0.01$ . Sample size (n) is reported above each bar.

**c-d.** Knockdown of eIF2 $\gamma$  kinases GCN2 and PEK alleviate impaired climbing (**c**) and activity (**d**) phenotypes in *Drosophila* pan-neuronally (nSyb-Gal4) expressing GR(1000) at 21 days post-eclosion. Error bars = SEM, Kruskal-Wallis with post-hoc Dunn's comparison to

controls \*  $p < 0.05$ , \*\*  $p < 0.01$ , \*\*\*  $p < 0.001$ , \*\*\*\*  $p < 0.0001$ . Sample size (n) is reported above each bar.

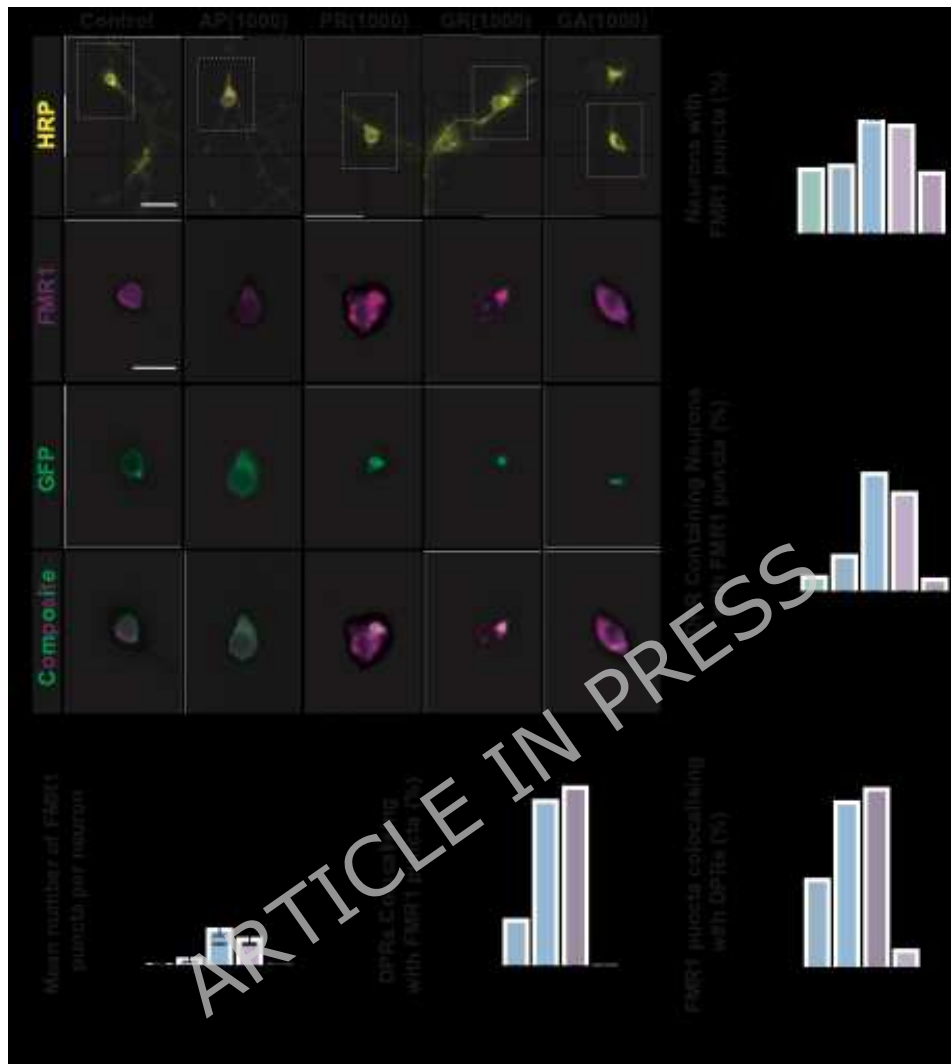


**Fig. 3. Pan-Neuronal Expression of Arginine Rich DPRs Leads to Accumulation of the Stress Granule marker FMR1 in *Drosophila* Neurons**

- a.** Representative micrographs of *Drosophila* primary neurons from flies pan-neuronally (nSyb-Gal4) expressing 1000-repeat DPRs, or an mCD8-GFP control. Neurons are labelled with the neuronal marker anti-HRP, anti-GFP (labelling GFP-tagged DPRs) and anti-FMR1. Scale bars = 10  $\mu$ m.
- b.** Quantification of the percentage of neurons within primary cultures pan-neuronally (nSyb-Gal4) expressing 1000-repeat DPRs, or an mCD8-GFP control, displaying FMR1

positive puncta. Error bars = SEM, Chi-Squared with Bonferroni correction \*  $p < 0.05$ . Sample size (n) is reported above each bar.

**c.** Quantification of the percentage of primary neurons displaying DPR aggregates, when pan-neuronally (nSyb-Gal4) expressing 1000-repeat DPRs, or an mCD8-GFP control, containing FMR1 positive puncta. Error bars = SEM, Chi-Squared with Bonferroni correction \*\*\*\*  $p < 0.0001$ . Sample size (n) is reported above each bar.

**d.** Quantification of the mean number of FMR1 positive puncta in primary neurons expressing (nSyb-Gal4) 1000-repeat DPRs, or an mCD8-GFP control. Sample size (n) is reported above each bar.

**e.** The percentage of DPR aggregates colocalising with FMR1 in primary neurons expressing (nSyb-Gal4) 1000-repeat DPRs, or an mCD8-GFP control. Sample size (n) is reported above each bar.

**f.** The percentage of FMR1 puncta colocalising with DPR aggregates in primary neurons expressing (nSyb-Gal4) 1000-repeat DPRs, or an mCD8-GFP control. Sample size (n) is reported above each bar.

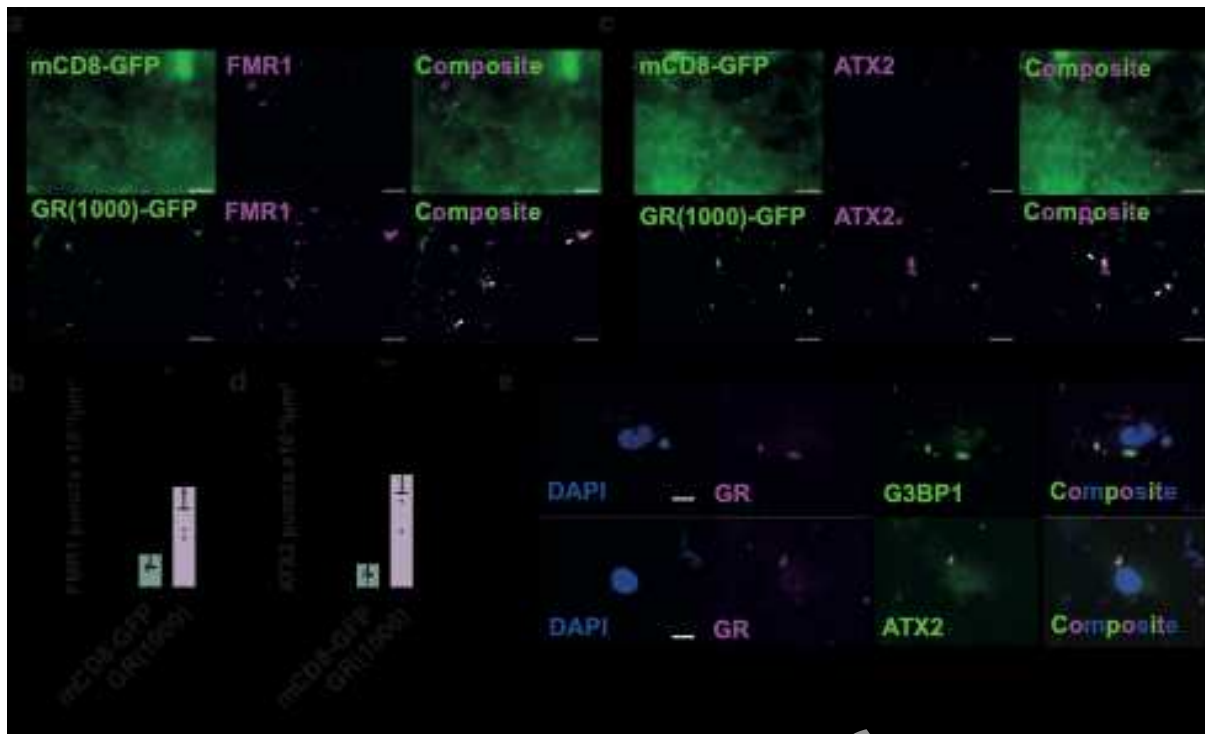


**Fig. 4. Accumulation of Stress Granule Markers and colocalisation with PolyGR in *Drosophila* brains and patient-derived motor neurons.**

**a.** Representative micrographs showing accumulation of FMR1 and PolyGR in the brains of *Drosophila* pan-neuronally (nSyb-Gal4) expressing GR(1000), or an mCD8-GFP control at 28 days post-eclosion, following heat stress (37 °C for 2 hours prior to dissection). Scale bars = 20  $\mu$ m.

**b.** Quantification of the number of FMR1 positive puncta in the brains of *Drosophila* pan-neuronally (nSyb-Gal4) expressing GR(1000), or an mCD8-GFP control at 28 days post-eclosion, following heat stress (37 °C for 2 hours prior to dissection). Error bars = SEM, unpaired T-test \*  $p < 0.05$ .

**c.** Representative micrographs showing accumulation of ATX2 and PolyGR in the brains of *Drosophila* pan-neuronally (nSyb-Gal4) expressing GR(1000), or an mCD8-GFP control at 28 days post-eclosion, following heat stress (37 °C for 2 hours prior to dissection). Scale bars = 20  $\mu$ m.

**d.** Quantification of the number of ATX2 positive puncta in the brains of *Drosophila* pan-neuronally (nSyb-Gal4) expressing GR(1000), or an mCD8-GFP control at 28 days post-

eclosion, following heat stress (37 °C for 2 hours prior to dissection). Error bars = SEM, unpaired T-test \*\* p < 0.01.

e. Representative micrographs showing colocalisation of PolyGR with stress granule markers G3BP1 and ATX2 in day 40 C9orf72 repeat expansion patient-derived motor neurons. Scale bars = 10  $\mu$ m.

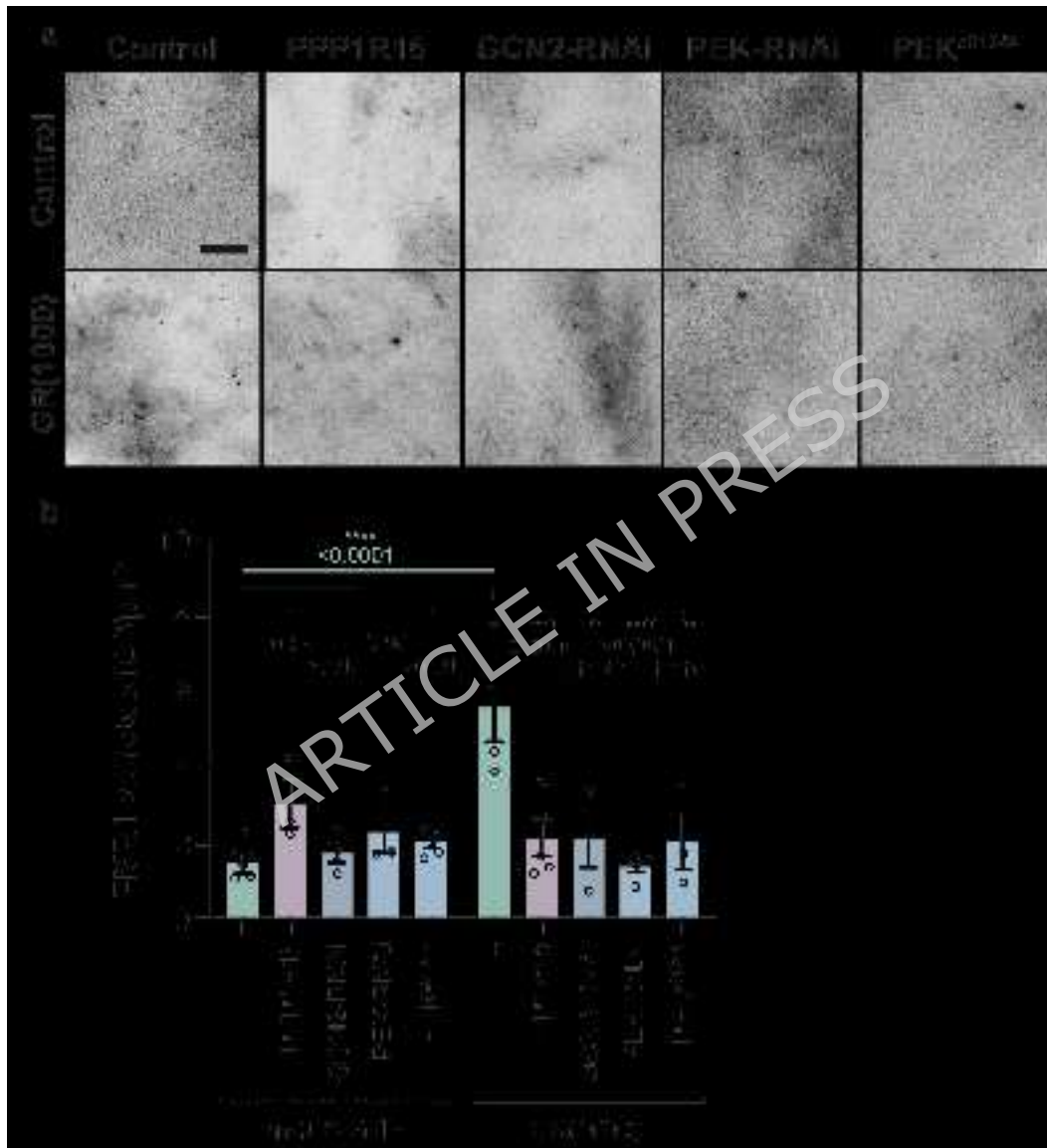


**Fig. 5. Inhibition of the integrated stress response reduces the number of FMR1 positive puncta observed in *Drosophila* pan-neuronally expressing GR(1000).**

**a.** Representative micrographs showing accumulation of FMR1 in the brains of *Drosophila* pan-neuronally (nSyb-Gal4) expressing GR(1000), or an mCD8-GFP control at 21 days post-eclosion. Scale bars = 25  $\mu$ m.

**b.** Quantification of the number of FMR1 positive puncta in the brains of *Drosophila* pan-neuronally (nSyb-Gal4) expressing GR(1000), or an mCD8-GFP control at 21 days post-eclosion. Error bars = mean  $\pm$  SEM. ANOVA with post-hoc Šídák's multiple comparison test, \*\*  $p < 0.01$ , \*\*\*  $p < 0.001$ , \*\*\*\*  $p < 0.0001$ .



**Fig. 6. Knockdown of ATX2 Alleviates Climbing Deficits in *Drosophila* GR(1000) Models**

**a.** Quantification of climbing speed in flies pan-neuronally (nSyb-Gal4) co-expressing 1000-repeat DPRs, or an mCD8-GFP control (Control), with either a Gal4 titration control (+ = mCD8-GFP), UAS-ATX2 or UAS-ATX2-RNAi, at 28 Days post-eclosion. Error bars = SEM, ANOVA with post-hoc Tukey test, \*\*\*\*  $p < 0.0001$ . Sample size (n) is reported above each bar.

**b.** Quantification of climbing speed in flies pan-neuronally (nSyb-Gal4) co-expressing GR(1000), or an mCD8-GFP control, with either a Gal4 titration control (mCD8-GFP) or UAS-ATX2-RNAi, at 7, 14, 21 and 28 Days post-eclosion. Error bars = SEM.

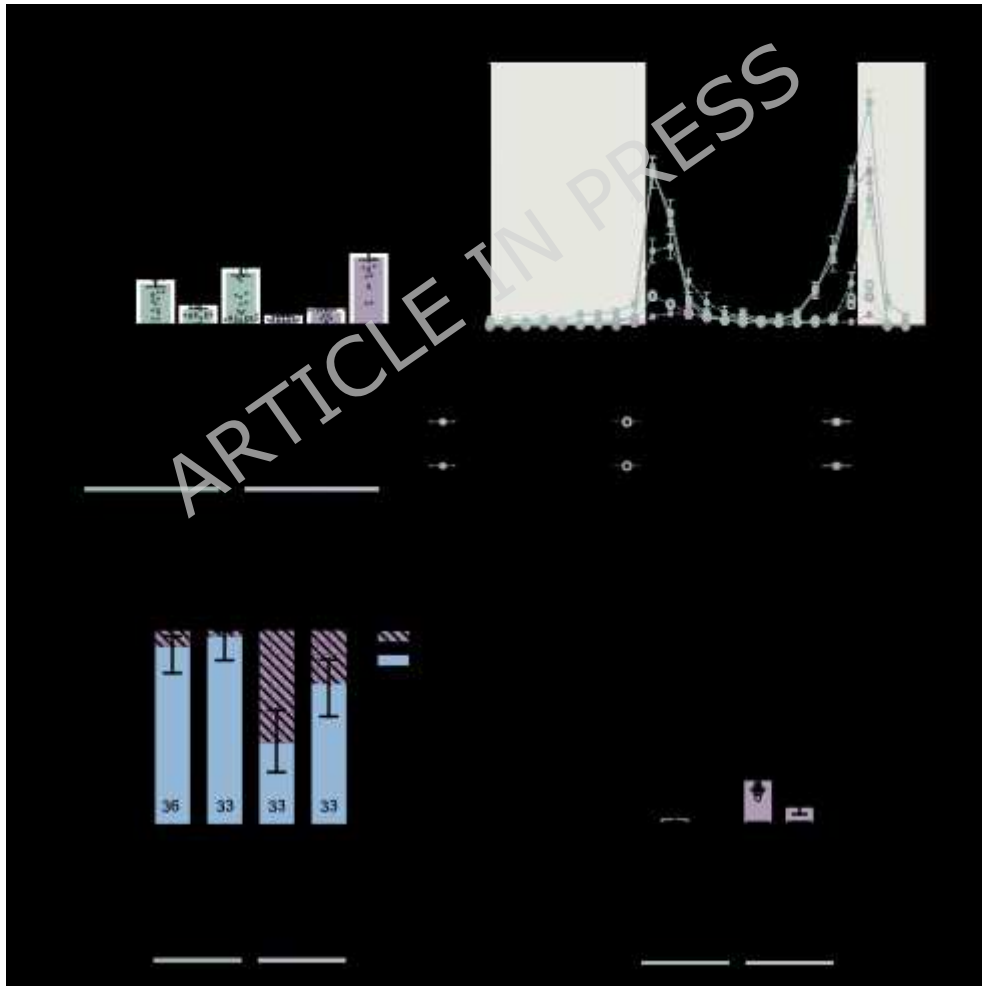


**Fig. 7. Knockdown of ATX2 Alleviates Activity and Seizure Phenotypes in *Drosophila* GR(1000) Models**

- a.** Quantification of activity (Moves made in 24 hours) in flies pan-neuronally (nSyb-Gal4) co-expressing GR(1000), or an mCD8-GFP control (Control), with either a Gal4 titration control (+ = mCD8-GFP), an RNAi control (UAS-mCherry-RNAi) or UAS-ATX2-RNAi<sup>1</sup>, at 28 Days post-eclosion. Error bars = SEM, Kruskal-Wallis with post-hoc Dunn's comparison to controls \*\*  $p < 0.01$ , \*\*\*\*  $p < 0.0001$ .
- b.** 24 hour actogram showing hourly activity (Moves) of flies pan-neuronally (nSyb-Gal4) co-expressing GR(1000), or an mCD8-GFP control (Control), with either a Gal4 titration control (+ = mCD8-GFP), an RNAi control (UAS-mCherry-RNAi) or UAS-ATX2-RNAi<sup>1</sup>, at 28 Days post-eclosion.
- c.** Quantification of the percentage of flies displaying seizure phenotypes following mechanical (vortex) stimulation in flies pan-neuronally (nSyb-Gal4) co-expressing GR(1000), or an mCD8-GFP control (Control), with either a Gal4 titration control (+ = mCD8-GFP) or UAS-ATX2-RNAi<sup>1</sup> at 28 Days post-eclosion. Error bars = SEM, Chi-Squared with Bonferroni correction \*  $p < 0.05$ , \*\*\*  $p < 0.001$ . Number of flies seizing is reported above each bar and flies not seizing within the bar.
- d.** Quantification of the length of seizures observed following mechanical (vortex) stimulation in flies pan-neuronally (nSyb-Gal4) co-expressing GR(1000), or an mCD8-GFP control (Control), with either a Gal4 titration control (+ = mCD8-GFP) or UAS-ATX2-RNAi<sup>1</sup> at 28 Days post-eclosion. Error bars = SEM, Kruskal-Wallis with post-hoc Dunn's comparison to controls \*\*  $p < 0.01$ , \*\*\*\*  $p < 0.0001$ .

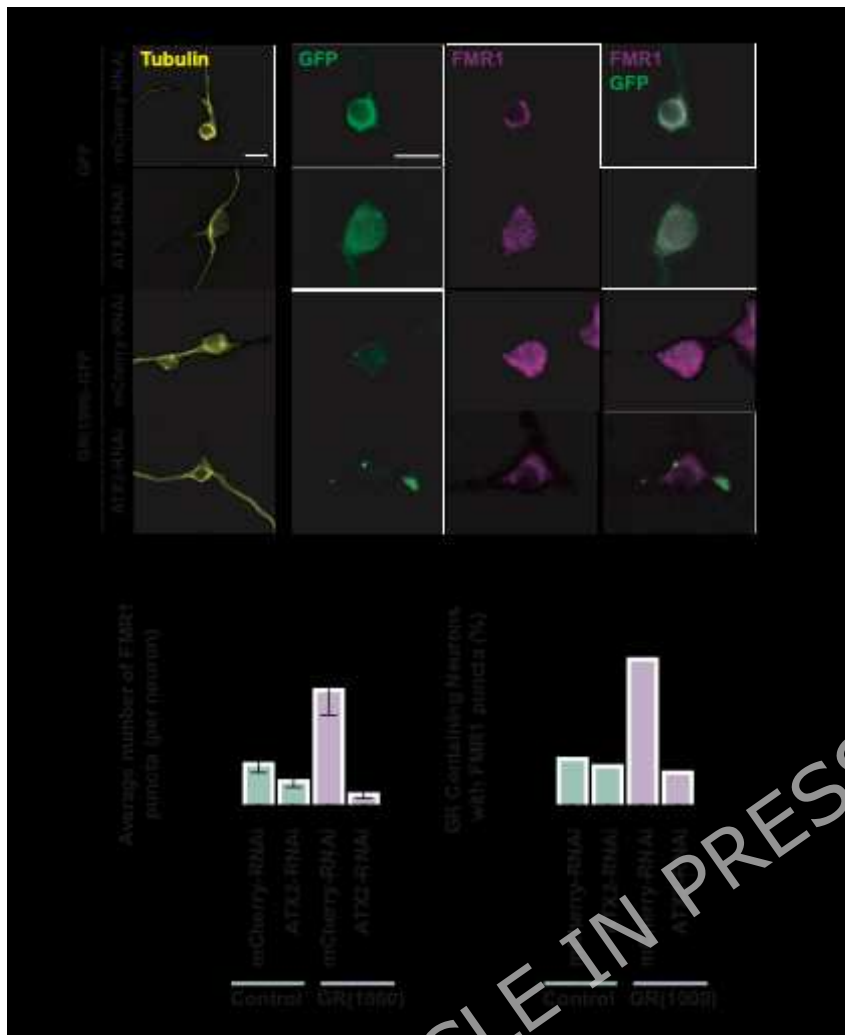


**Fig. 8. Knockdown of ATX2 reduces the number of FMR1 positive Stress Granules observed in GR(1000) expressing primary Neurons**

**a.** Representative micrographs of *Drosophila* primary neurons from flies pan-neuronally (nSyb-Gal4) co-expressing GR(1000), or an mCD8-GFP control, with either an RNAi control (UAS-mCherry-RNAi) or UAS-ATX2-RNAi<sup>1</sup>. Scale bars = 5  $\mu$ m.

**b.** Quantification of the mean number of FMR1 positive puncta in primary neurons from flies pan-neuronally (nSyb-Gal4) co-expressing GR(1000), or an mCD8-GFP control, with either an RNAi control (UAS-mCherry-RNAi) or UAS-ATX2-RNAi<sup>1</sup>. Error bars = SEM, Kruskal-Wallis with post-hoc Dunn's comparison to controls \*\*\* p < 0.001. Sample size (n) is reported above each bar.

**c.** Quantification of the percentage of neurons pan-neuronally (nSyb-Gal4) co-expressing GR(1000), or an mCD8-GFP control, with either an RNAi control (UAS-mCherry-RNAi) or

UAS-ATX2-RNAi<sup>1</sup> containing FMR1 positive puncta. Error bars = SEM, Chi-Squared with Bonferroni correction \*\*\*\*  $p < 0.0001$ . Sample size (n) is reported above each bar.

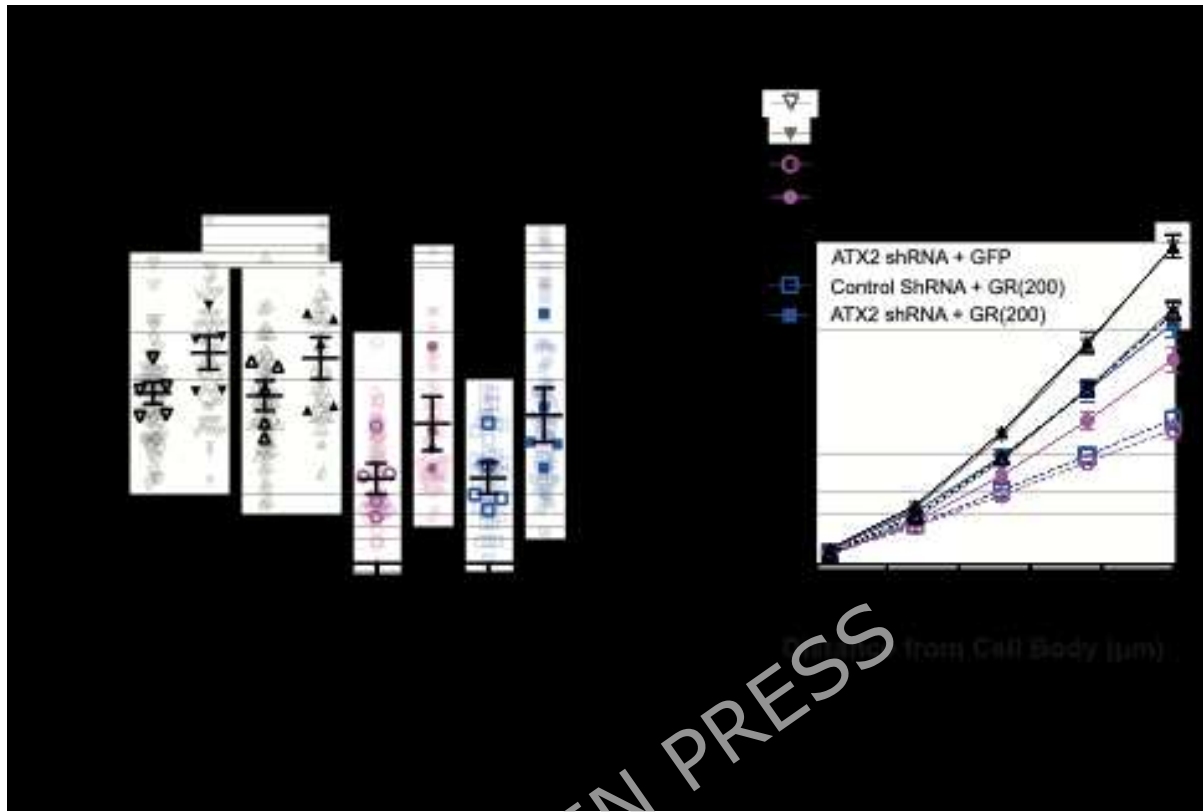


**Fig. 9. Knockdown of ATX2 ameliorates neuronal morphology defects in mouse primary neurons transduced with PolyGR**

**a.** Quantification of the dendritic complexity (total number of intersections) of mouse primary neurons co-transduced with either GFP, GR100 or GR200 and either a control scrambled shRNA or ATXN2-shRNA. Shaded/transparent shapes represent individual cells with solid/opaque shapes showing the mean of each biological replicate. Statistics were performed on the means of biological replicates, 2-way ANOVA with post-hoc Tukey test, \*  $p < 0.05$ .

**b.** Quantification of the dendritic complexity (cumulative number of intersections) of mouse primary neurons co-transduced with either GFP, GR100 or GR200 and either a control scrambled shRNA or ATXN2-shRNA.

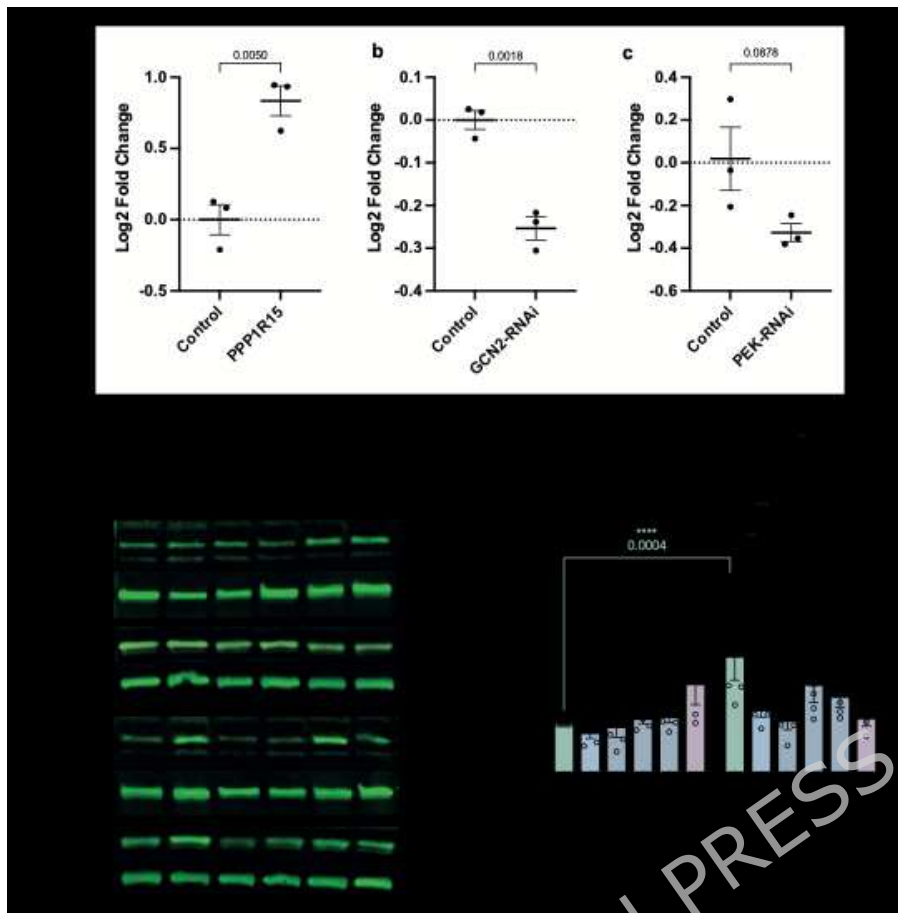


**Fig. S1.**

**a.** QRT-PCR quantification of PPP1R15 in the heads of *Drosophila* pan-neuronally (nSyb-Gal4) overexpressing UAS-PPP1R15. Error bars = SEM. Paired t-test.

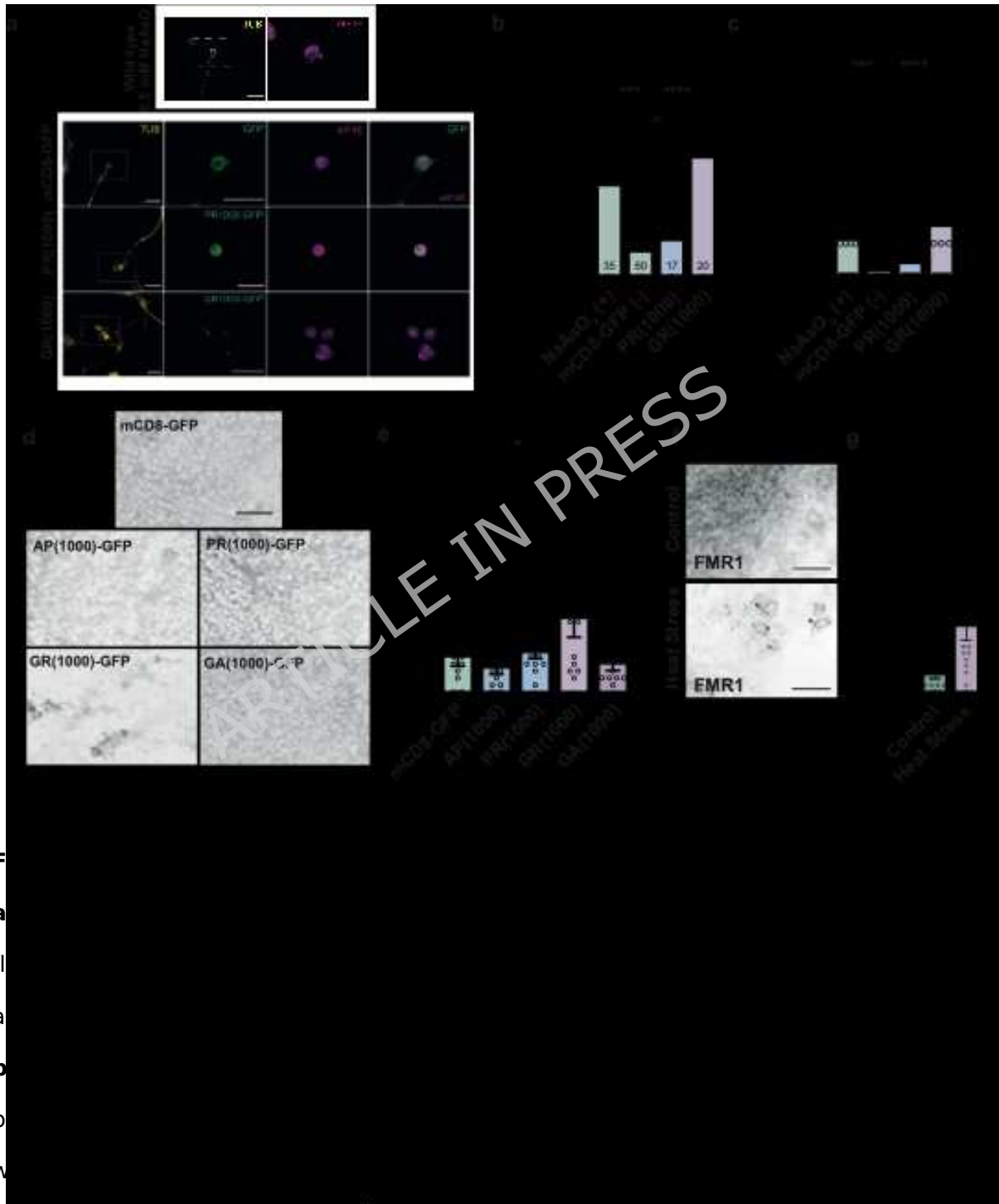
**b.** QRT-PCR quantification of GCN2 in the heads of *Drosophila* pan-neuronally (nSyb-Gal4) expressing UAS-GCN2-RNAi. Error bars = SEM. Paired t-test.

**d.** QRT-PCR quantification of PEK in the heads of *Drosophila* pan-neuronally (nSyb-Gal4) expressing UAS-PEK-RNAi. Error bars = SEM. Paired t-test.

**d.** Representative western blots showing levels of eIF2, p-eIF2 and ̑-tubulin in the heads of *Drosophila* pan-neuronally (nSyb-Gal4) co-expressing GR(1000), or an mCD8-GFP control, with PPP1R15, GCN2-RNAi, PEK-RNAi, PEK<sup>e01744</sup>, ATX2-RNAi<sup>1</sup> or an mCherry-RNAi control.

**e.** Quantification of the p-eIF2/eIF2 ratio in the heads of *Drosophila* pan-neuronally (nSyb-Gal4) co-expressing GR(1000), or an mCD8-GFP control, with PPP1R15, GCN2-RNAi, PEK-RNAi, PEK<sup>e01744</sup>, ATX2-RNAi or an mCherry-RNAi control. Error bars = mean  $\pm$  SEM.

ANOVA with post-hoc Šídák's multiple comparison test, \*\*  $p < 0.01$ , \*\*\*  $p < 0.001$ , \*\*\*\*  $p < 0.0001$ . n = shown on bars



Squared with Bonferroni correction \*\*\*  $p < 0.001$ , \*\*\*\*  $p < 0.0001$ . n = shown on bars, N = 3.

- c.** Quantification of the number of eIF4E puncta observed in primary cultures from *Drosophila* pan-neuronally (nSyb-Gal4) expressing GR(1000), PR(1000), or an mCD8-GFP control and wild-type primary neurons treated with sodium arsenite (NaAsO<sub>2</sub>). Error bars = SEM, Kruskal-Wallis with post-hoc Dunn's comparison to controls \* p < 0.05, \*\* p < 0.01, \*\*\* p < 0.001, \*\*\*\* p < 0.0001. n = shown on bars, N = 3.
- d.** Representative micrographs showing accumulation of FMR1 in the brains of *Drosophila* pan-neuronally (nSyb-Gal4) expressing 1000-repeat DPRs, or an mCD8-GFP control at 28 days post-eclosion. Scale bars = 20 μm.
- e.** Quantification of the number of FMR1 positive puncta in the brains of *Drosophila* pan-neuronally (nSyb-Gal4) expressing 1000-repeat DPRs, or an mCD8-GFP control at 28 days post-eclosion. Error bars = SEM, ANOVA with post-hoc Dunnett's comparison to controls \* p < 0.05.
- f.** Representative micrographs showing accumulation of FMR1 in the brains of wild-type *Drosophila* following heat-stress (2h, 37°C) at 5 days post-eclosion. Scale bars = 20 μm.
- g.** Quantification of the number of FMR1 positive puncta in the brains of wild-type *Drosophila* following heat-stress (2h, 37°C) at 5 days post-eclosion. Error bars = SEM, unpaired T-test \*\* p < 0.01.

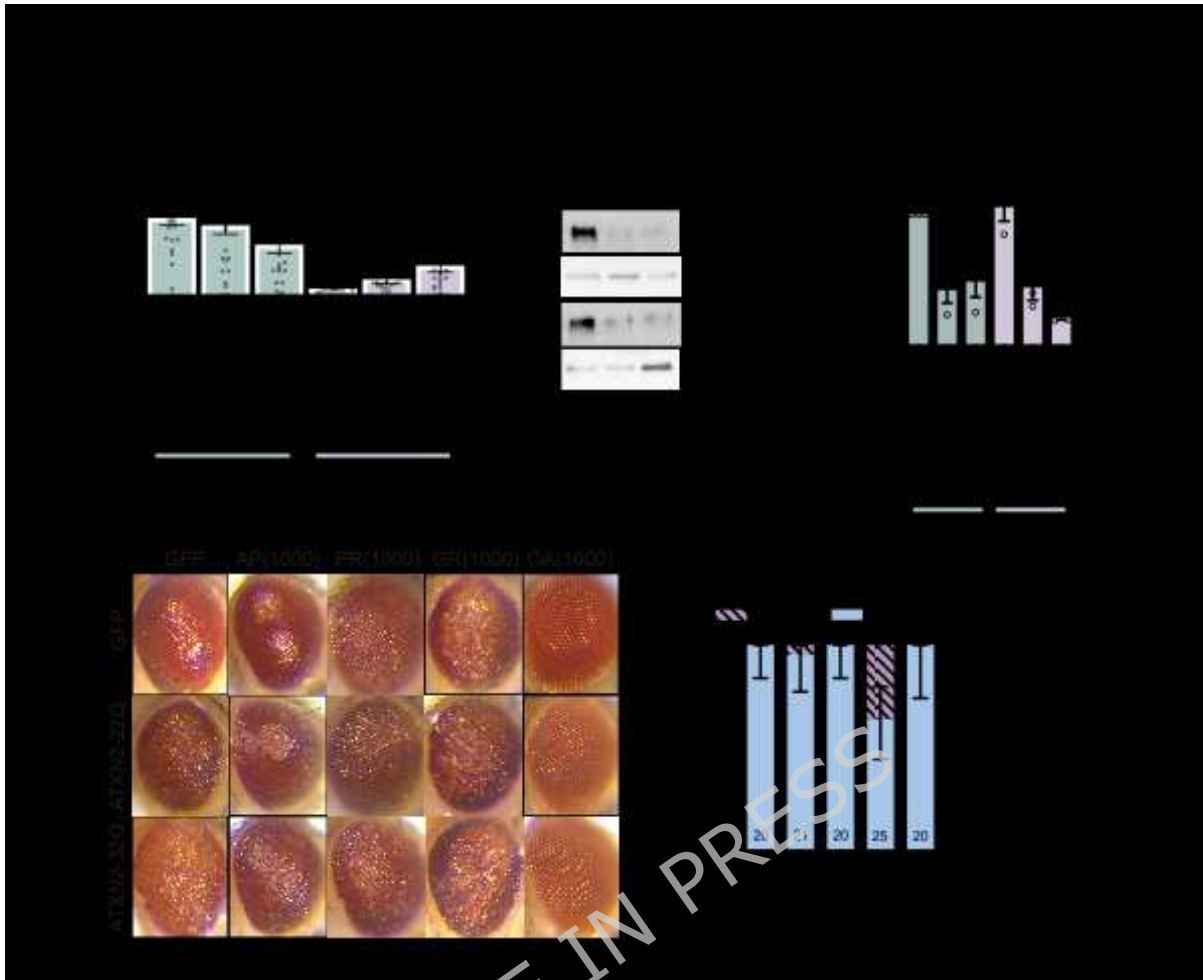


**Fig. S3.**

**a.** Quantification of climbing speed in flies pan-neuronally (*nSyb-Gal4*) co-expressing *GR(1000)*, or an *mCD8-GFP* control (Control), with either an RNAi control (*UAS-mCherry-RNAi*) or *UAS-ATX2-RNAi*, at 28 Days post-eclosion. Error bars = SEM, Kruskal-Wallis with post-hoc Dunn's comparison to controls \*  $p < 0.05$ .

**b.** Representative western blots showing the abundance of *ATX2* in the heads of flies pan-neuronally (*nSyb-Gal4*) co-expressing *GR(1000)*, or an *mCD8-GFP* control (Control), with two independent *ATX2* RNAi lines. 28 days post-eclosion.

**c.** The relative abundance of *ATX2* in the heads of flies pan-neuronally (*nSyb-Gal4*) co-expressing *GR(1000)*, or an *mCD8-GFP* control (Control), with two independent *ATX2* RNAi lines. Normalised to tubulin. 28 days post-eclosion. Error bars = SEM, ANOVA with post-hoc Šidák's comparison between groups \*\*  $p < 0.01$ , \*\*\*  $p < 0.001$ .

- d.** Expression of human Ataxin-2 with normal (22Q) and intermediate (32Q) polyglutamine expansions does not modify DPR toxicity when expressed in the *Drosophila* eye.
- e.** Quantification of the percentage of flies pan-neuronally (nSyb-Gal4) expressing 1000-repeat DPRs, or an mCD8-GFP control displaying seizure phenotypes following mechanical (vortex) stimulation at 14 Days post-eclosion. Error bars = SEM, Chi-Squared with Bonferroni correction \*\*  $p < 0.01$ .

**Table. S1. Šídák's multiple comparisons test, 7 vs 21 DPE**

Genotype	Adjusted p value		
	eIF2 $\beta$	p-eIF2 $\beta$	p-eIF2 $\beta$ :eIF2 $\beta$ ratio
Control	0.9997	>0.9999	>0.9999
AP1000	>0.9999	0.9991	0.9075
PR1000	0.9837	0.8805	>0.9999
GR1000	0.4885	>0.9999	0.2628
GA1000	0.9993	0.5977	0.5750